NASA CONTRACTOR REPORT

NASA CR-1941

THIN FILM OXYGEN PARTIAL PRESSURE SENSOR

by J. J. Wortman, J. W. Harrison, H. L. Honbarrier, and J. Yen

Prepared by
RESEARCH TRIANGLE INSTITUTE
Research Triangle Park, N.C.
for Langley Research Center

NATIONAL AERONAUTICS AND SPACE ADMINISTRATION • WASHINGTON, D. C. • JANUARY 1972

1. Report No.	2. Government Accession No.	3. Recipient's Catalog No.
NASA CR-1941		

4. Title and Subtitle	5. Report Date
Thin Film Oxygen Partial Pressure Sensor	January 1972
	6. Performing Organization Code

7. Author(s)	8. Performing Organization Report No.
J. J. Wortman, J. W. Harrison, H. L. Honbarrier, J. Yen	
	10. Work Unit No.

9. Performing Organization Name and Address	11. Contract or Grant No.
Research Triangle Institute Research Triangle Park, North Carolina	NAS1-9827
	13. Type of Report and Period Covered
12. Sponsoring Agency Name and Address	Contractor Report
National Aeronautics and Space Administration Washington, D.C. 20546	14. Sponsoring Agency Code

15. Supplementary Notes

16. Abstract

This report details the development of a laboratory model oxygen partial pressure sensor using a sputtered zinc oxide thin film. The film is operated at about 400° C through the use of a miniature silicon bar. Because of the unique resistance versus temperature relation of the silicon bar, control of the operational temperature is achieved by controlling the resistance. A circuit for accomplishing this is described.

The response of sputtered zinc oxide films of various thicknesses to oxygen, nitrogen, argon, carbon dioxide and water vapor caused a change in the film resistance. Over, a large range film conductance varied approximately as the square root of the oxygen partial pressure. The presence of water vapor in the gas stream caused a shift in the film conductance at a given oxygen partial pressure.

A theoretical model is presented to explain the characteristic features of the zinc oxide response to oxygen.

17. Key Words (Suggested by Author(s))	18. Distribution Statement
Partial Pressure Sensor, Zinc Oxide Thin Film Miniaturized Heater	Unclassified - Unlimited

19. Security Classif. (of this report)	20. Security Classif. (of this page)	21. No. of Pages	22. Price*
Unclassified	Unclassified	90	$3.00

*For sale by the National Technical Information Service, Springfield, Virginia 22151

CONTENTS

LIST OF ILLUSTRATIONS

LIST OF ILLUSTRATIONS (continued)

LIST OF ILLUSTRATIONS (continued)

LIST OF TABLES

LIST OF SYMBOLS

A	proportionally constant relating O_2 surface concentration to O_2 partial pressure in ambient gas
A_o	dimensionless constant relating relative change in resistance to difference in activation energies
B	desorption velocity constant, number per unit area per second
E_A	adsorption activation energy, eV
E_{AR}	activation energy characteristics of resistance R, electron volts
E_D	desorption activation energy, eV
E_{A1}, E_{A2}	activation energies for adsorption of molecules type 1 and type 2, respectively, eV
E_{D1}, E_{D2}	activation energies for desorption of molecules type 1 and type 2, respectively, eV
k	Boltzmanns constant, 8.6×10^{-5} eV/°k
K_R	constant of proportionality relating resistance, in ohms, to reciprocal carrier density
K_1, K_2	equilibrium constants for chemical reactions
m_1, m_2	mass of molecules type 1 and type 2, respectively
n_c	number of surface sites per unit area covered by adsorbed materials
n_o	carrier density prior to annealing, number per cubic meter
n_s	number of surface sites per unit area
N_s	number of surface sites for adsorption
p	partial pressure of a gas, N/m^2
p_0	an "initial" pressure, N/m^2
p_{02}	O_2 partial pressure in ambient air

LIST OF SYMBOLS (Con'd)

p_T	Total pressure
R	Resistance, ohms
T	temperature, °K
T_G	gas temperature, °K
T_s	surface temperature, °K
u	adsorption velocity, number per unit area per second
u'	desorption velocity, number per unit area per second
V,V(p)	interaction energy at pressure p, electron volts (eV)
V_o	interaction energy at initial pressure p_0, electron Volts (eV)
Δn	change in carrier density
ΔR	change in resistance
$\Delta\mu$	change in free energy in a chemical reaction, eV
Θ	fraction of surface covered by adsorbed gas particles
Θ_{02}	fraction of surface sites occupied by O_2
Θ_1,Θ_2	fraction of surface covered by molecules of type 1 and type 2, respectively
σ	condensation coefficient for adsorption

THIN FILM OXYGEN PARTIAL PRESSURE SENSOR

By J. J. Wortman, J. W. Harrison, H. L. Honbarrier and J. Yen†
Research Triangle Institute

SECTION I

INTRODUCTION

The purpose of this study has been to develop and evaluate a thin film zinc oxide partial pressure sensor. The main thrust of the program has been to demonstrate the practicality of utilizing sputtered zinc oxide films in the sensing element combined with a miniaturizing semiconductor heater.

Previous work [Ref. 1,2] has demonstrated that zinc oxide films, when held at an elevated temperature, are sensitive to oxygen partial pressure and can potentially be used as a partial pressure sensor. In the previous studies, the zinc films were formed by first vacuum evaporating pure zinc onto a suitable ceramic substrate which was followed by a high temperature oxidation step. Although these films were sensitive they were difficult to fabricate in a reproducible manner. Another difficulty in the early study was the lack of a suitable miniaturized heater for the film. Pearson [Ref. 3,4] has since demonstrated that a miniature semiconductor heater made from a material such as silicon could be used to produce the needed temperatures. Pearson not only demonstrated that a semiconductor rod could be used to heat the film but he also demonstrated that the rod resistance could be used as a measure of the temperature of the film and hence greatly simplify the total sensor system.

As a part of the present study, a sputtering technique has been developed and demonstrated. Zinc oxide films have been deposited with various thicknesses on several types of substrates. These films were characterized relative to their properties as a function of film thickness, annealing temperature and environment, and sensitivity to various environments as a function of temperature. In addition to film characterization, effort was expended on the development of suitable electrical contacts to the zinc oxide which would withstand both a high temperature environment and a long time operation.

The work of Pearson on the miniaturized heater was extended to develop the criteria needed to choose material parameters and electrical contacts for the semiconductor heater. A suitable insulating material was found and evaluated for electrically isolating the zinc oxide film from the semiconductor heater.

†North Carolina State University, Raleigh, North Carolina

The above mentioned technologies were combined into working sensor elements and evaluated. In addition a complete sensor unit, including electronics and control elements, was fabricated into an oxygen partial pressure sensor and tested.

The results of the study indicate that the combination of the sputtered zinc oxide films and the semiconductor heater can be used to form a miniaturized oxygen partial pressure sensor. Although development work will be required, this study shows that miniaturized, low cost oxygen partial pressure sensors are possible for numerous applications such as hospitals, space suits, diving suits, etc.

SECTION II

SPUTTERED ZINC OXIDE FILMS

Sputtering Process

The sensors prepared on this contract used zinc oxide films which were sputtered from a ZnO source. Experiments were performed to determine the best operating conditions for obtaining repeatable films. The equipment and procedures developed for this purpose are described below.

Apparatus. - A schematic diagram of the process equipment connections is given in Figure 1. The basic sputtering unit was composed of a vacuum chamber which could be pumped down to a pressure level of about $1.33 \times 10^{-4} N/m^2 (10^{-6}$ torr), an r-f power supply which operated at a fixed frequency of 13.5 megahertz, a tunable impedance matching network between the power supply and the vacuum chamber, and combination gas purifier/regulator for controlling the leak rate of desired gases into the chamber. Photographs of the assembly are shown in Figure 2.

The substrate holder consisted of a copper block with built-in heating elements and a water/gas cooling system. Although the distance between the target of the sputtering source and the substrate holder could be adjusted, a fixed distance of 7.5 cm was maintained throughout the sputtering runs made in the present work. The sputtering source was a zinc oxide target of 12.5 cm diameter.

The inert gas used for the sputtering plasma was ultra-high purity grade (99.99%) argon. The chamber pressure was measured with an ionization type vacuum gauge and a pirani type vacuum gauge.

For the initial runs the substrates used were quartz slides. These facilitated handling for inspections to determine film quality and thickness measurements to determine the deposition rate. Later ceramic coated silicon bars were used, as will be described subsequently in Section III of this report. Film quality was checked using a high power optical microscope and a scanning electron microscope. Film thickness was measured using standard interference techniques on an optical microscope.

Operating procedures. - A typical sputtering operational cycle consisted of the following steps:

1. Chamber and substrate cleanup

2. Chamber pump down and load prematching.

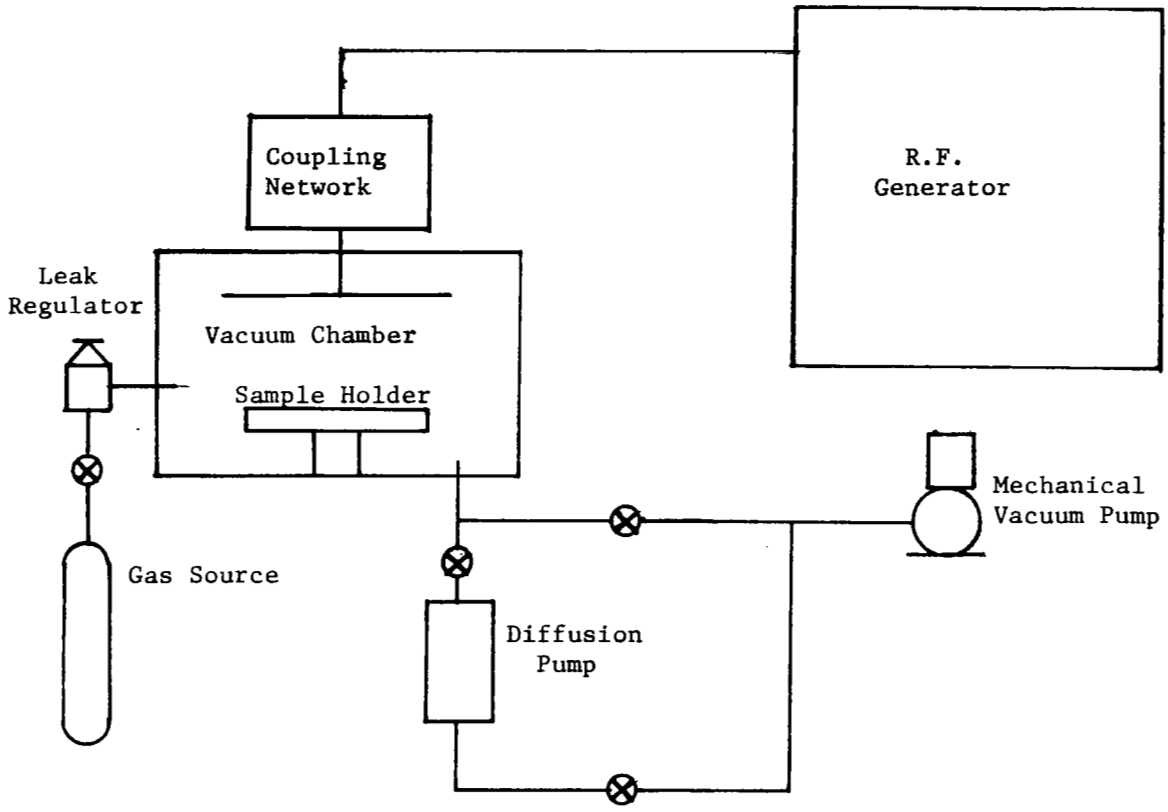

Figure 1. Schematic Diagram of Sputtering Apparatus Used to Obtain ZnO Films for Partial Pressure Sensors.

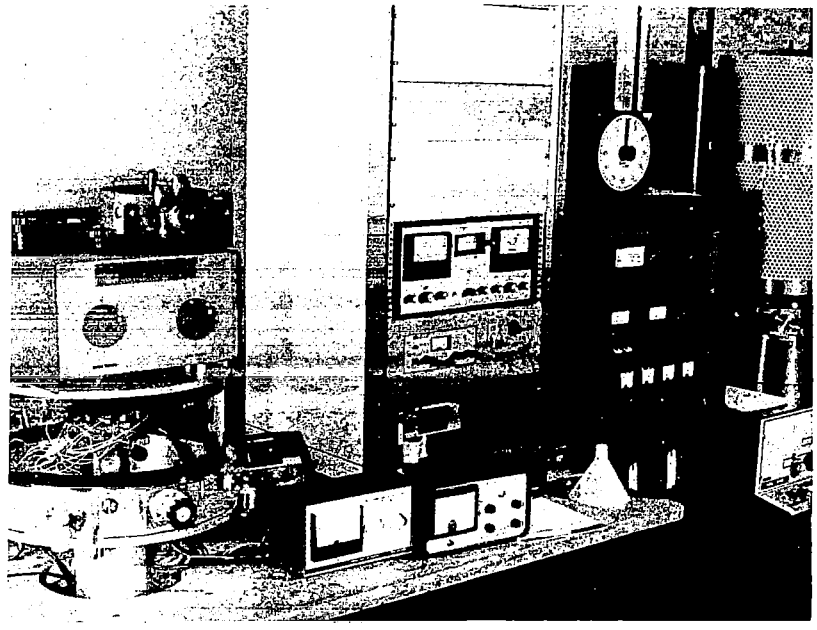

Figure 2. Sputtering Unit Used to Deposit ZnO Films. The Block Used for Measurement of Film Electrical Resistance is Shown in Place in the Vacuum Chamber.

3. Substrate loading and chamber pump down.

4. Inert gas flow setting and chamber pressure adjustment.

5. RF power application and impedance matching to obtain desired glow characteristics.

6. Deposition.

7. Shutdown and sample removal.

The details of each of these steps are given in the following paragraphs.

Standard cleaning procedures for vacuum equipment were used. Materials deposited on the previous run were carefully removed from all interior surfaces by scouring and sanding where necessary. Organic solvents were used to remove any oils and greases from vacuum exposed surfaces of the chamber and the substrate materials.

In order to match the load to the r-f generator and condition the chamber for a deposition, a load prematching step was used. The chamber was sealed and roughed down with a mechanical pump. Then a diffusion pump was used to bring the chamber pressure down to a base level of $1.33 \times 10^{-4} N/m^2 (10^{-6}$ torr). Typically the system was pumped down overnight. Inert gas was introduced and the pressure adjusted to obtain a glow. Then the system was sputtered by ZnO without any substrates. During this operation the load matching network was adjusted to obtain maximum power transfer. In addition to cleaning out the system and matching the load to the generator, this step aided in obtaining a good deposition of ZnO on the substrate holder indicating the best location for substrate placement for subsequent sputtering.

Following placement of the substrates on the substrate holder, the chamber was sealed and pump down started. After roughing down by a mechanical vacuum pump, a diffusion pump was used to reduce the pressure to the $1.33 \times 10^{-4} N/m^2 (10^{-6}$ torr) base level. Typically only two hours was required to reach the base level.

For argon flow setting, the supply pressure of argon to the inert gas leak/purification assembly was set at about $2.8 \times 10^5 N/m^2$ and the leak rate flow set at 10 cc/min. The high vacuum valve in the diffusion pump line was set to achieve an equilibrium pressure of $0.667\ N/m^2$ (5 millitorr), a level shown to be satisfactory for low sputtering rates by previous experience.

As suggested by the manufacturer, the r-f power supply was adjusted for an output of 200 watts. Then the chamber pressure was increased to

attain a plasma in the argon. Usually the plasma would glow at around 4 N/m^2 (30 millitorr). Then the pressure was reduced back to the desired low sputtering rate level of 0.667 N/m^2 (5 millitorr). Following pressure stabilization the matching network was adjusted to match the geometry dependent load to the r-f generator. Following this the shutter over the substrates was removed to start the deposition. Final matching adjustments were made at this time. The pre-matching procedure allowed a rapid final adjustment, which resulted in better repeatability of the film growth rate and properties.

Deposition time and film thickness. - Due to the geometrical restriction of the ZnO target size, quartz substrates were cut into 6.25 mm squares and were placed within a 7.5 cm diameter circle at the center of the substrate holder. For a one hour deposition time the film thickness measured roughly 360 nm. A linear variation with deposition time was assumed to estimate the thickness of films obtained in runs of less than one hour length, i.e.

film thickness (nanometers) = 0.1 × deposition time (second)

It was noted that deposition times of less than 600 seconds did not yield reproducible results.

Substrate temperature. - During the deposition tap water was continuously circulated through the copper block supporting the substrates. This was done to maintain the substrates near room temperature even though heat was being transferred from the plasma to the substrates. No provision was made to monitor the substrate temperature during the sputtering operation.

Measurement Procedure

Measurement arrangement. - Equipment and instruments for measuring the variation of film resistance with temperature and gaseous environment variations was connected as shown schematically in Figure 3. To provide ohmic contacts to the film, two parallel strips of liquid bright platinum were painted on opposite edges of rectangular sample films. These were fired in air at 673°K. Either pressure contacts were used or gold leads were bonded to the platinum strips. The samples, on their quartz substrates were mounted on a copper block which could accomodate three samples. This block was equipped with cartridge heaters and had chromel-alumel thermocouples embedded for control and monitoring of the block temperature. A photograph of the sample block is shown in Figure 4.

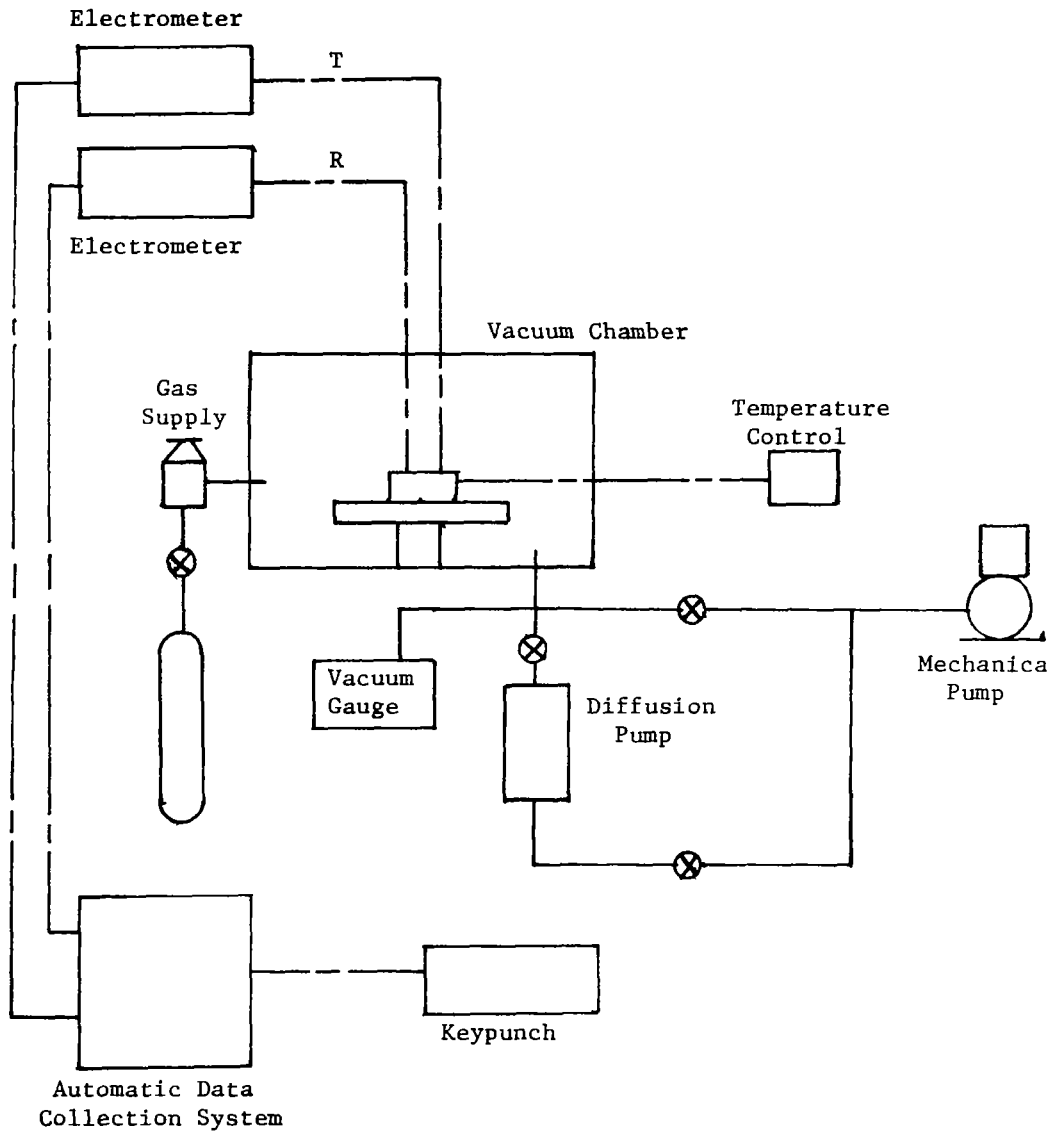

Figure 3. Measurement Arrangement.

Figure 4. Copper Block Used for Maintaining Sample Temperature While Making Electrical Measurements. Contact to Platinum Bands on the ZnO Films was Made through Screw-down Pressure Contacts in Slotted Bars on the Top of the Block.

The sputtering chamber was used as an environmental test chamber. By controlling the input leak rate of gas and the pumping rate in a manner similar to that used to control the sputtering pressure, any pressure between $1.33 \times 10^{-3} N/m^2$ and $1.0 \times 10^{5} N/m^2$ of the gases used in the tests could be maintained constant during the measurements. Gas pressure was measured with either vacuum gauges or thermocouple gauges, depending upon the pressure level used.

For sample resistance measurements, commercial electrometers were used. An electronic voltmeter was used to measure the output of a thermocouple monitoring the surface temperature of the copper block holding the samples. The output signals of these meters were monitored by an automatic data sampling system which transformed the analog signals to digital data punched into computer cards, giving four place resolution. Sampling interval was one minute. This data was processed on a digital computer. Representative points were selected at random from this data to obtain a plot of the logarithm of sample resistance versus either time, temperature or oxygen partial pressure.

Measurement procedure. - The properties of two sets of films were measured. In each set samples of 90 nm, 180 nm and 360 nm thickness were used. The sets were designated Y and G. After measurements had been made on these samples of both sets in the "as grown" state (not annealed), the samples of set G were annealed by heating to 873°K in 100% ambient for 24 hours. The annealed films were re-designated Ga. The measurements of gas and temperature effects were repeated for the set Ga.

The environmental test procedure for each set of samples was carried out as follows:

1. Temperature effects at constant pressure. On each of these tests the temperature of the samples was raised to 673°K. At the constant gas pressures given below the temperature was decreased to room temperature and then heated back to 673°K while resistance as a function of temperature was measured. The gas ambients used were:

   a. Air at $1.33 \times 10^{-3} N/m^2 (10^{-5}$ torr)

   b. Oxygen (0_2) at $1.33 N/m^2$ (0.01 torr)

   c. Oxygen 0_2 at $13.3 N/m^2$ (0.10 torr)

   d. Oxygen (0_2) at $1.33 N/m^2$ (1.0 torr)

e. Nitrogen (N_2) at 13.3 N/m^2(0.1 torr)

f. Nitrogen (N_2) at 133 N/m^2(1.0 torr)

g. Argon (Ar) at 13.3 N/m^2(0.1 torr)

h. Argon (Ar) at 133 N/m^2(1.0 torr)

2. Effect of type gas at constant temperature and pressure.

   a. Switch from N_2 to O_2 at 133 N/m^2(1.0 torr) total pressure. After stabilizing, switch from O_2 to N_2.

   b. Repeat at a total pressure of 13.3 N/m^2(0.1 torr)

   c. Change to another temperature and repeat (a) and (b).

Data and Analysis

Data from the measurements made on annealed and unannealed ZnO films sputtered on quartz substrates is presented and analyzed in subsequent paragraphs. One of the main features of the behavior observed was the practically linear variation of the logarithm of the film resistance with reciprocal temperature at constant oxygen pressure in the range from about 300°K to 673°K. In this range, to a good approximation the resistance can be represented by

$$R = R_o \exp\left(E_R/kT\right)$$

where R_o is a temperature independent constant, k is Boltzmann's constant and E_R is called the activation energy for the process.

It was found that the value of R_o and E_R depend upon the oxygen content in the gas ambient of the ZnO films. Both parameters increase with increasing oxygen content. It was also found that when the films were annealed in an atmosphere containing oxygen, the values of R_o and E_R for a given pressure of oxygen were both significantly increased. The following model seems consistent with this behavior.

Zinc oxide, unless otherwise intentionally doped, is usually found to be an n-type semiconductor with the donors assumed to be interstitial zinc atoms [Ref. 2]. The model used to explain the data reported here assumes that the increase in resistance is due to trapping of conduction band electrons at the surface of the zinc oxide by adsorbed oxygen. The form of the oxygen, O_2 or O, is immaterial for the aspects of the model

discussed below in connection with the data. The concept of a surface is extended in the present model to include the possibility of small pores or crevices. This is done in order to explain the longer time response of thicker films.

In the tests reported the films were heated at a constant rate of 0.1°K/sec and cooled at a constant rate of 0.05°K/sec. The films were not strictly at thermal equilibrium when each measurement was made. However, most of the data reported and discussed below was taken at the relatively slow cooling rate. Consequently, the use of equilibrium concepts to draw conclusions from the measurements should be justified.

Effect of Temperature. - Data which was collected and stored on cards was processed on a digital computer using a program which plotted the data. A typical example is shown in Figure 5. The vertical scale is proportional to reciprocal temperature, 1000/°K, and the horizontal scale is $\log_{10}R$. The characters 2, 3, and 4 are data points corresponding to films of different thickness. From plots similar to this, data points were taken to make the plots presented subsequently in this section of the report.

Figure 6 shows the variation of resistance with temperature for films of 90 nm, 180 nm and 360 nm thickness under oxygen (O_2) at 1.33 N/m^2. When the oxygen pressure was increased to 13.3 N/m^2, the resistance varied with temperature as shown in Figure 7. With another increase in oxygen pressure, this time 133 $N/m^2 O_2$, the resistance of samples of films at the three different thicknesses varied with temperature as shown in Figure 8. Each curve can be approximated by a straight line of slope proportional to E_R, which will be termed an "activation energy". All of the values of E_R calculated from these straight line approximations are less than 1 eV. One electron volt (eV) is equivalent to 1.60×10^{-19} Joule in the International System of units. When discussing electronic transition energies it is convenient to use the eV as the unit of energy. According to Kröger [Ref. 5, page 691], the energy band gap of ZnO is given by

$$E_G = 3.2 - 10^{-3}T \qquad (1)$$

where T is the temperature in °K. This relation gives E_G = 2.9 eV at 300°K and E_G = 2.53 eV at 673°K, the upper limit of the temperature measurements. The influence of oxygen partial pressure on the slopes will be discussed in a subsequent section.

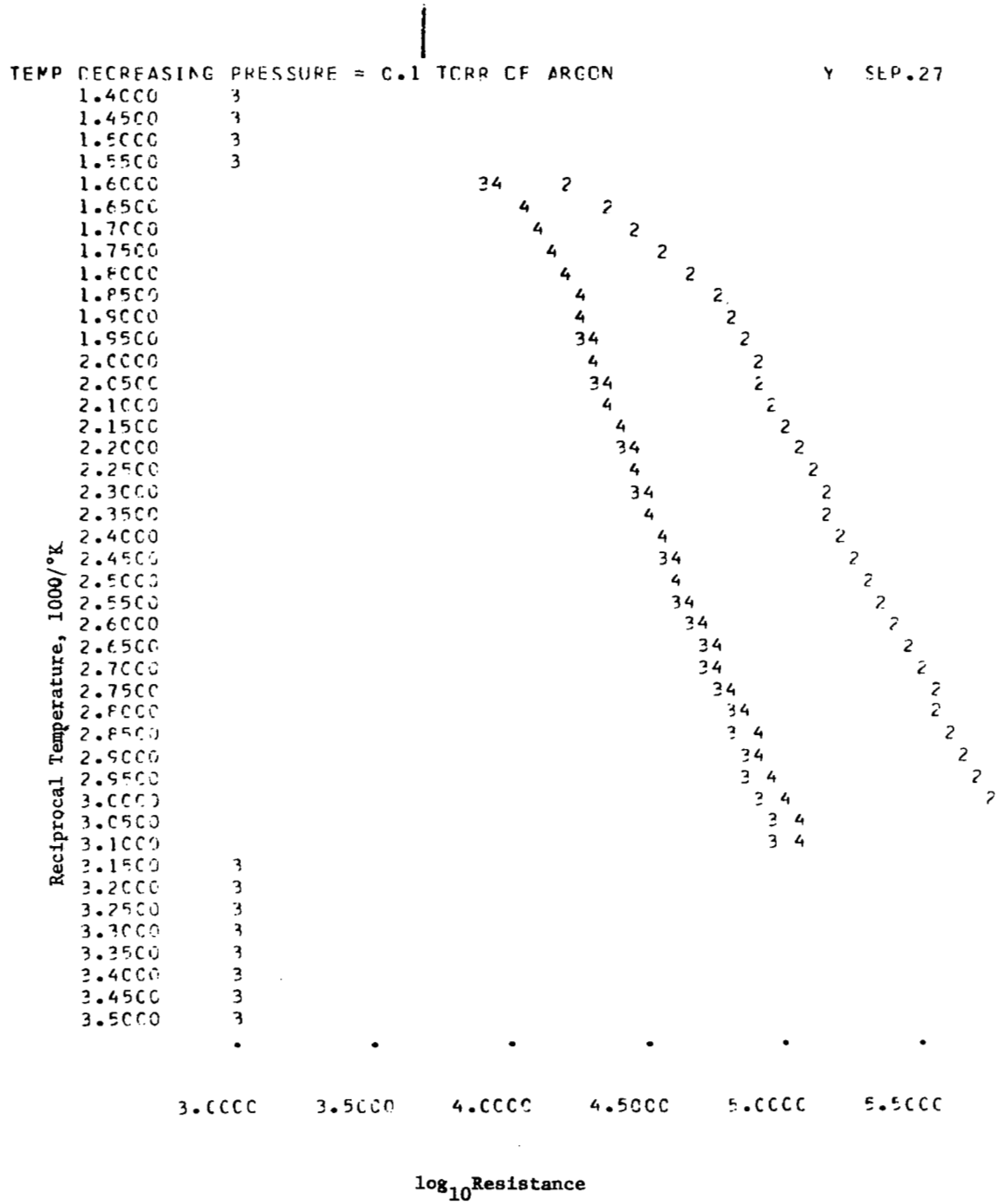

Figure 5. Computer Plot of Data Taken on 90 nm, 180 nm and 360 nm Films Under 13.3 N/m^2 (0.1 torr) Pressure of Argon.

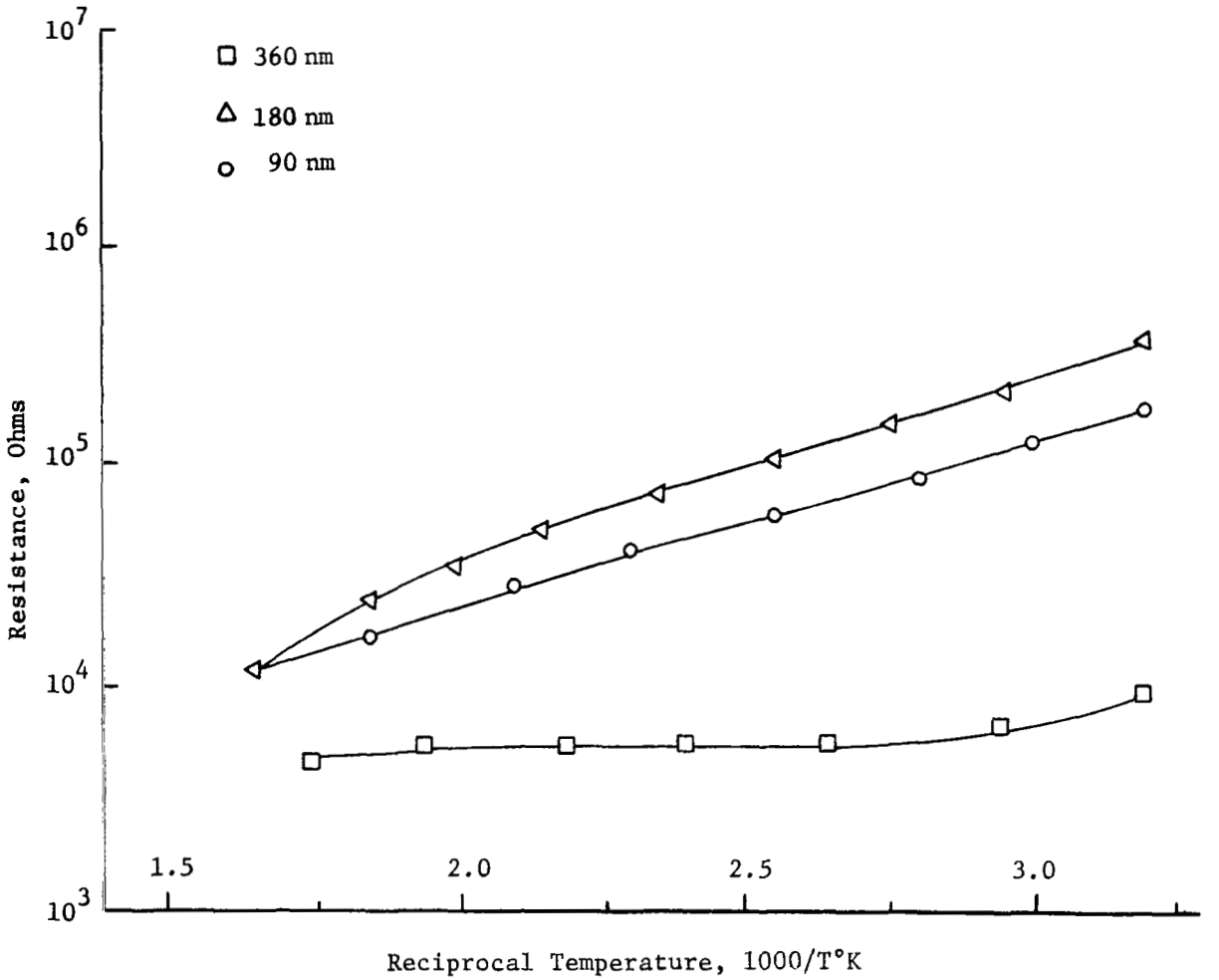

Figure 6. Resistance As a Function of Reciprocal Temperature for Three ZnO Film Thickness. Data Taken at a Constant Cooling Rate under 1.33 N/m^2(0.01 torr) Oxygen Pressure.

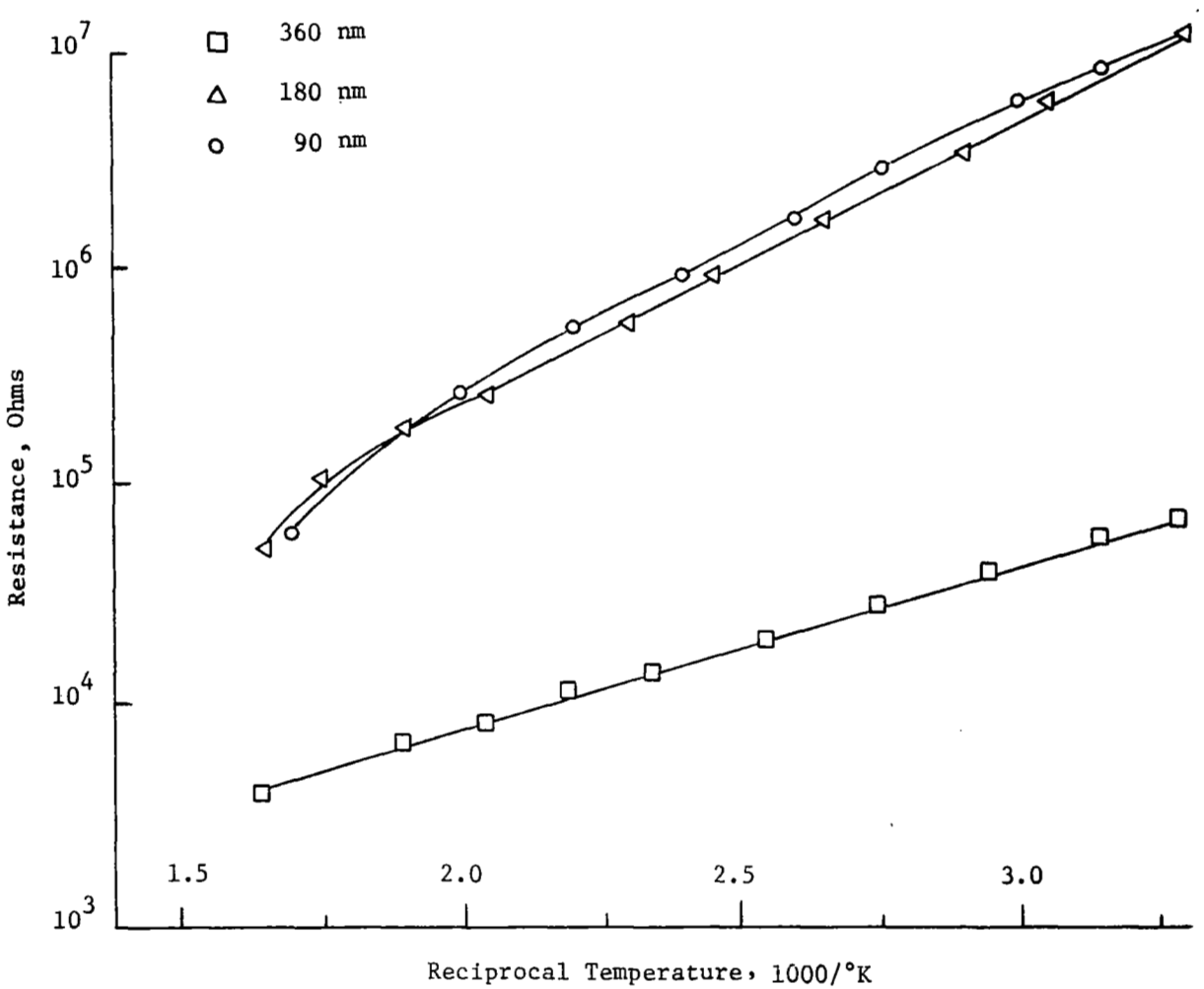

Figure 7. Resistance As a Function of Reciprocal Temperature for Three ZnO Film Thicknesses. Data Taken at a Constant Cooling Rate under 13.3 N/m^2(0.1 torr) Oxygen Pressure.

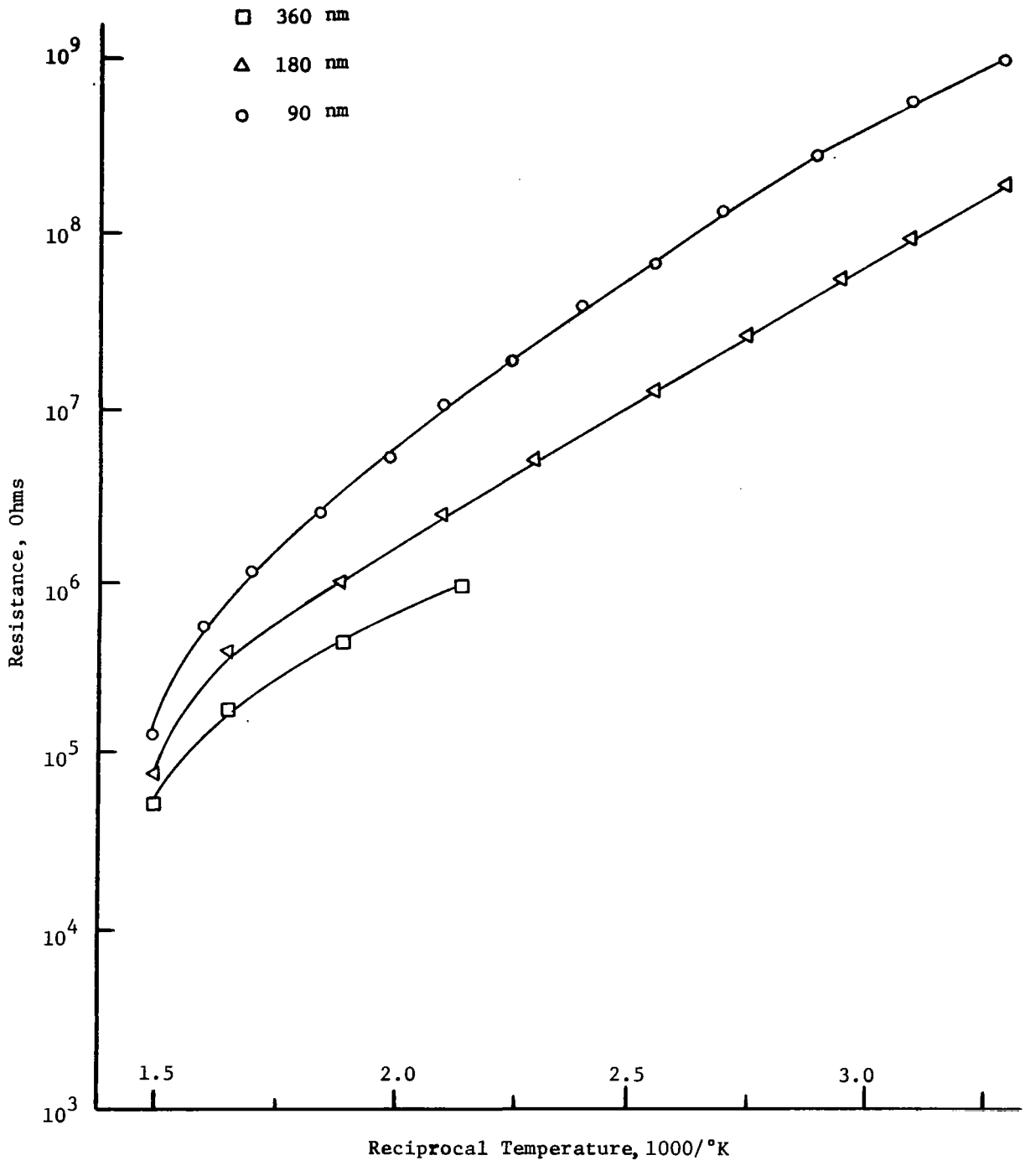

Figure 8. Resistance As a Function of Reciprocal Temperature for Three ZnO Film Thicknesses. Data Taken at a Constant Cooling Rate under 133 N/m^2(1 torr) Oxygen Pressure.

The effect of temperature cycling is demonstrated in Figure 9 for a film of 180 nm thickness. Initially the film was heated to 673°K under the specified partial pressure of O_2 without making any measurement. Then the films were cooled at a constant rate of about 0.05°K/sec and the resistance measured. During another heating cycle at about 0.1°K/sec rate the resistance was measured again as a function of temperature.

The somewhat different slopes for heating and cooling of the log R versus 1/T curves of Figure 9 indicate that there are some quasi-irreversible effects. These are not as drastic as those reported by Tischer [Ref. 6] or Royal, et al. [Ref. 2]. However, these workers subjected their samples to higher temperatures prior to descreasing back to room temperature. In the present measurements, after the initial heat up, the film resistance variation was found to be reversible and reproducible. The reproducibility is shown in Figure 10 for an 180 nm film at 133 N/m^2(1 torr) pressure of O_2.

Effect of oxygen pressure. - The data presented in Figure 9 also can be used to aid in the delineation of the mechanism causing resistance changes in the ZnO film with changes in the ambient oxygen partial pressure. To do this the curves are approximated by straight lines. The lowest cooling curve is for an air pressure of $1.33 \times 10^{-3} N/m^2$($10^{-5}$ torr) or about $2.66 \times 10^{-4} N/m^2$($2 \times 10^{-6}$torr) of O_2. To a good approximation this is the "zero pressure" curve for O_2. It represents the bulk behavior of film resistance versus temperature. The slope of the lowest curve must be related to the ionization energy required to create mobile charge carriers in the semiconductor. The slope of the "zero pressure" curve corresponds to an activation energy of about 0.047 eV. This represents ionization from a shallow level. The first ionization level for interstitial zinc or for an oxygen vacancy is given by Kröger [Ref. 5, page 691] as 0.05 eV. This is very close to the activation energy observed. The slope observed on the heating curve for an oxygen partial pressure of $2.66 \times 10^{-4} N/m^2$ (2×10^{-6} torr) is 0.104 eV which indicates some change has taken place in the nature of the donor.

The resistance at pressure p for oxygen and temperature T is given by

$$R(p,T) = R(o,T) + \Delta R(p,T) \tag{2}$$

or

$$R(p,T) = R_o + \Delta R \tag{3}$$

For $\Delta R >> R_o$

$$R(p,T) \simeq \Delta R \tag{4}$$

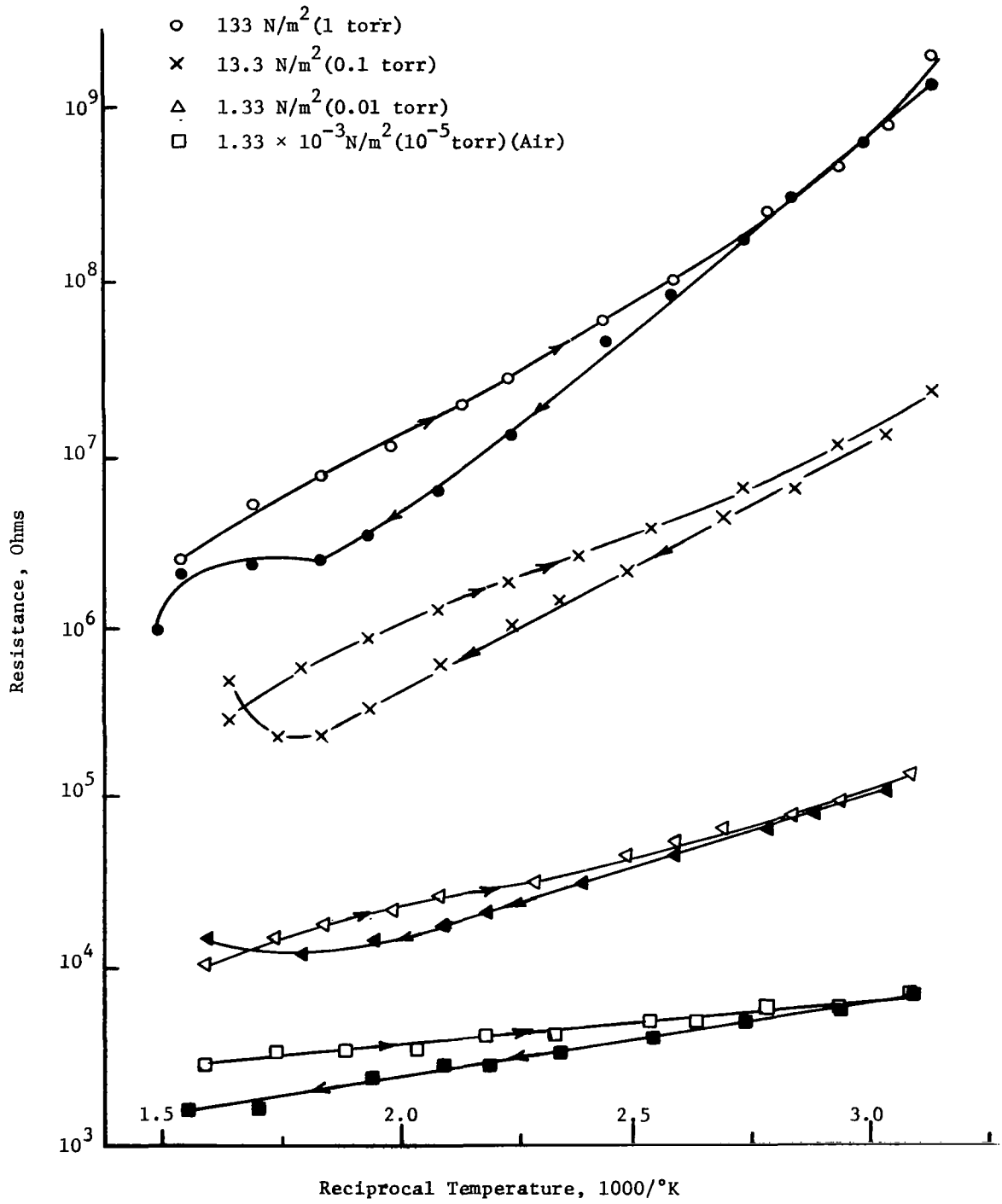

Figure 9. Resistance As a Function of Reciprocal Temperature for 180 nm ZnO Film. Data Taken at Constant Cooling and Heating Rates Under the Oxygen Pressures Indicated.

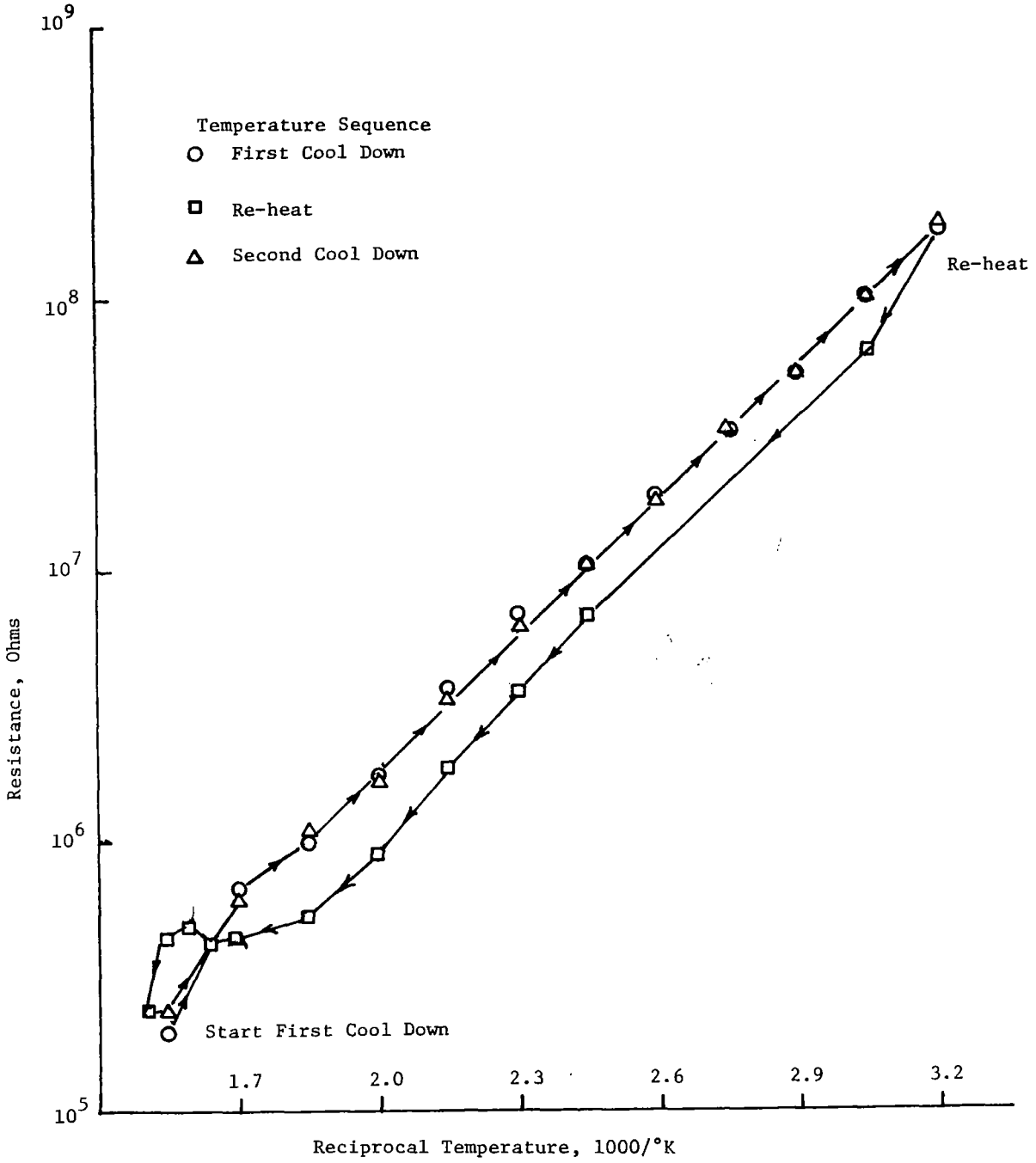

Figure 10. Resistance As a Function of Reciprocal Temperature for 180 nm ZnO Film Showing Reproducible Behavior Following Re-heating. Data Taken at 133 N/m^2(1 torr) Pressure of Oxygen.

This condition is fulfilled by the change in resistance for p = 13.3 N/m^2 (0.1 torr) of O_2, which is about two orders of magnitude larger than R_o, and for p = 133 N/m^2 (1.0 torr) of O_2, which is about three orders of magnitude larger than R_o.

The activation energy for p = 13.3 N/m^2 (0.1 torr) of O_2 is about 0.20 eV and for p = 133 N/m^2 (1.0 torr) is about 0.31 eV.

If it is assumed that the change in resistance at a constant temperature, T, is due only to a change in the number of carriers free to move in the material under the influence of an electric field, then

$$R_o = K_R/n_o \tag{5}$$

$$R = K_R/n = K_R/n_o - \Delta n \tag{6}$$

$$\Delta R = R-R_o = K_R\left(\frac{1}{n_o-\Delta n} - \frac{1}{n_o}\right) \tag{7}$$

$$\Delta R = K_R\Delta n/(n_o-\Delta n)n_o \tag{8}$$

$$\frac{\Delta R}{R_o} = \Delta n/(n_o-\Delta n) = \frac{\Delta n/n_o}{1-\Delta n/n_o} \tag{9}$$

$$\frac{\Delta n}{n_o} = \frac{\Delta R/Ro}{1+\Delta R/Ro} \tag{10}$$

In these equations n_o represents the initial free carrier density (number per cubic meter) and Δn the change in free carrier density. The constant K_R depends upon the geometry of the sample, the charge per carrier and the mobility of the carriers. The quantity $\ell n(\Delta R/R_o)$ has a slope proportional to the difference in the activation energies associated with R and R_o. Call this difference V,

where

$$V = E_R - E_{R_o} \ . \tag{11}$$

Now

$$\frac{\Delta R}{R_o} = A_o \exp V/kT \tag{12}$$

Therefore

$$\frac{\Delta n}{n_o} = \frac{A_o e^{V/kT}}{1 + A_o e^{V/kT}} = \frac{1}{1 + \frac{1}{A_o} e^{-V/kT}} \tag{13}$$

This result can be interpreted in the following manner. The ratio of the change in carrier concentration at temperature T and pressure p to the carrier concentration at T with p = o, given by (13) is given by the probability of an equilibrium coverage at p,T. The right hand side represents this probability. The energy V(p) can be interpreted as an interaction energy between adsorbed oxygen species. At a given coverage there is a spreading caused by repulsion between adsorbed species. If these adsorbed molecules (O_2) or atoms (O) are mobile to some extent, there is a tendency to depopulate the surface as the temperature is raised due to repulsive forces developed as the adsorbed species approach each other. At low pressure the surface population is low enough so that such encounters are not frequent. Raising the pressure, raises the density of adsorbates, giving an enhanced possibility of encounter as the temperature is raised. The surface population is assumed to be identical with the number of carriers depleted from the conduction band. Hence the equality (13).

The factor exp (-V/kT) may be regarded as a "crowding" factor. The factor $1/A_o$ should depend upon the form of the isotherm for the surface when crowding is ignored. The isotherm choice must be based on more evidence than is available in Figure 9. The choice will be discussed in Section III of this report when reviewing the data obtained on ZnO films in a miniature sensor configuration.

The values of the activation energies formed for two sets of films with two thickness, 90 nm and 180 nm, are given in Table 1 below:

TABLE 1. ACTIVATION ENERGY FOR ZnO FILMS

	Thickness 90 nm		
	Thermal Activation Energy (eV)		
P, N/m^2	Y	G	% Variation
1.33	0.142	0.129	5.5%
13.3	0.212	0.237	5.75%
133	0.343	0.346	0.7%

TABLE 1. ACTIVATION ENERGY FOR ZnO FILMS - Continued

	Thickness 180 nm		
P, N/m^2	Y	G	% Variation
1.33	0.120	0.157	5%
13.3	0.208	0.232	5.5%
133	0.283	0.295	1.05%

The agreement between sets for a given thickness is better than one might expect and is reasonable between the two different thicknesses used.

If this data is plotted as

$$\log V = m \log p + \log C \tag{14}$$

the slope obtained is approximately m = 0.25. This gives

$$V = V_o(P/P_o)^{1/4}. \tag{15}$$

This weak dependence upon pressure indicates that the repulsive forces involved are of relatively short range. The effects of such interactions on the fractional coverage, θ, of available adsorption sites have been discussed by Trapnell [Ref. 7, p. 99-100] and Peierls [Ref. 8].

To summarize, an increase in the partial pressure of oxygen in contact with a zinc oxide film which has not been annealed increases the magnitude of the resistance. The size of the change depends upon the temperature of the film. This may be explained by a model which allows for the interaction of adsorbed oxygen in such a manner that the heat of adsorbtion decreases with increasing coverage (increasing ambient partial pressure of oxygen). A decrease of the heat of adsorption with increasing coverage is a well known phenomenon. See, for example, Trapnell [Ref. 7, Chap. 6].

Effects of Annealing. - When the ZnO films are annealed at a high temperature, isobaric curves of log R versus 1/T are shifted upward, i.e. resistance of the film at a given temperature is significantly increased. Also the slope of the isobaric curves, which is proportional to the activation energy E_R, is significantly increased. The results of measurements on un-annealed, and subsequently annealed films are

presented in Table 2. This data includes measurements made under nitrogen and air as well as oxygen. The influences on film resistance of gases other than oxygen will be discussed in a subsequent paragraph. It is sufficient to note at this point that under nitrogen the slope of the log R versus 1/T curve increased by a factor of from two to three due to annealing.

Annealing for these films was carried out by overnight heating at 873°K with 100% O_2 gas flowing over the film. As can be seen from the data in Table 2, the slope of the log R versus 1/T curve decreases as thickness increases for un-annealed films. For the annealed films,

TABLE 2

ACTIVATION ENERGIES (electron volts)

Pressure (N/m^2)	Annealed Film			Un-annealed Film		
	Air	N_2	O_2	Air	N_2	O_2
			90 nm Thick			
1.33×10^{-3}	0.286			0.086		
13.3		0.295	0.569		0.145	0.237
133					0.131	0.347
			180 nm Thick			
1.33×10^{-3}	0.295			0.067		
13.3		0.342	0.327		0.106	0.231
133					0.100	0.295
			360 nm Thick			
1.33×10^{-3}	0.315			0.035		
13.3		0.345	0.380		0.076	0.132
133			0.428		0.0501	0.195

however, the slope for the 180 nm film is somewhat smaller than that for the 360 nm film at 13.3 N/m^2 of O_2.

Figure 11 shows a plot of log R versus 1/T data for an 180 nm film with O_2 pressure as a parameter for an un-annealed and subsequently annealed film. Here the increase in slope due to increased activation energy is very noticeable.

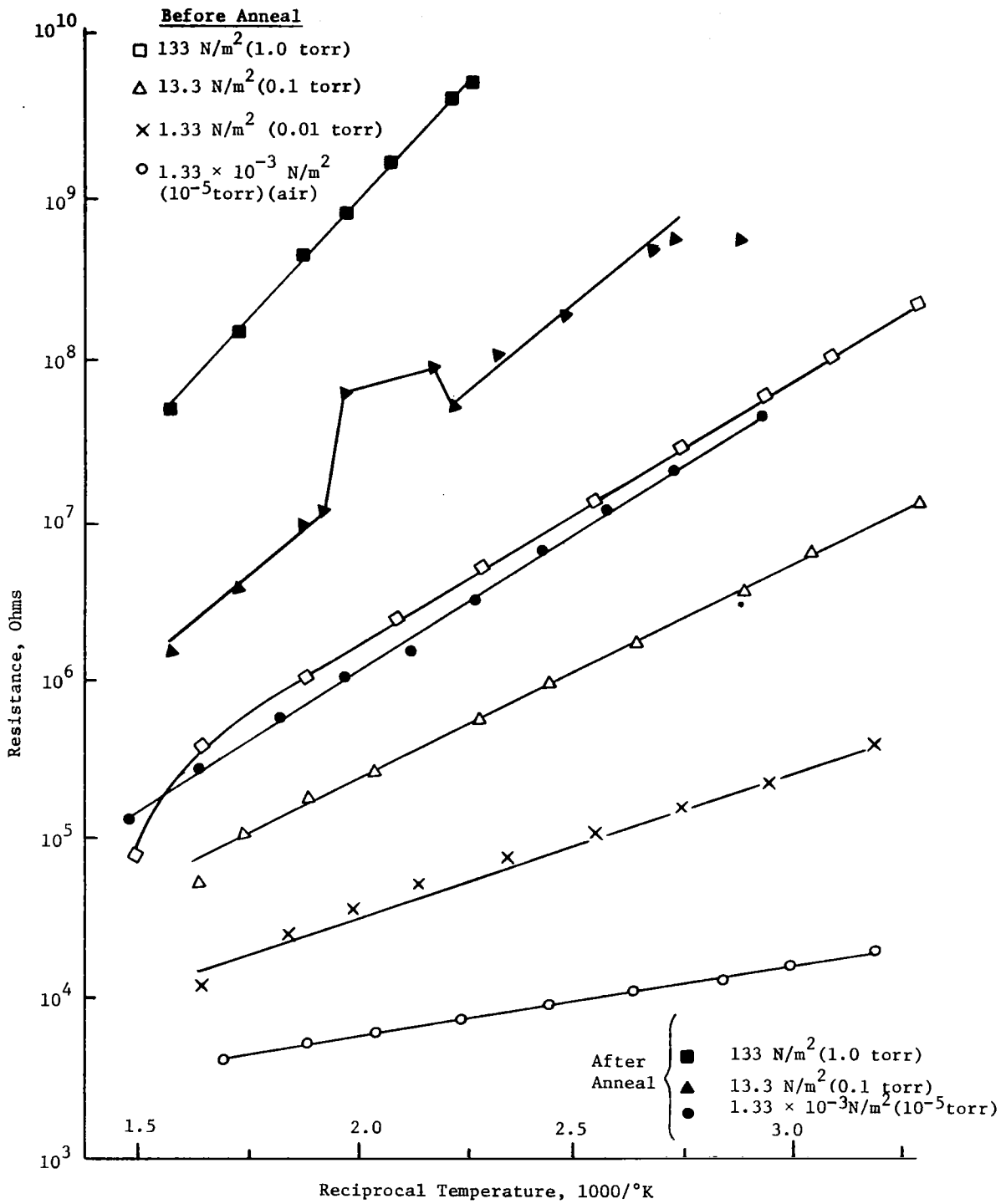

Figure 11. Resistance As a Function of Reciprocal Temperature for 180 nm ZnO Film at Oxygen Pressures Indicated, Showing the Effects of Annealing.

The broken curve for the annealed sample under 13.3 N/m^2 0_2 pressure occured when the scale was switched on the electrometer measuring film resistance. Changing the scale factor changes the voltage applied to the sample by the electrometer for the resistance measurement.

The argument was presented earlier that the slope of the log R versus 1/T plot for unannealed films at $1.33 \times 10^{-3} N/m^2$ of air was close enough to "zero pressure" conditions to yield the ionization energy of a donor in bulk ZnO which was taken as due to interstitial zinc atoms. If the same argument is made in the case of annealed films, the conclusion must be made that the nature of the donor has changed. The increase in resistance at a given temperature also indicates that the number of mobile charge carriers, presumed to be conduction band electrons, has decreased significantly.

From the data in Table 2, the activation energy of the hypothesized donor species is approximately 0.30 eV. This energy is lower than the 0.5 eV given by Kröger [Ref. 5, page 691] for the second ionization energy of interstitial zinc. The slope energy of about 0.30 eV is equivalent to 28.9 kJoule/mole. One possible mechanism which would account for such a donor species is a high degree of oxygen adsorption brought on by annealing in an atmosphere of appreciable oxygen content. The initial heat of adsorption for chemisorbed species is usually large, on the order to 83 to 420 kJoule per mole, according to Trapnell [Ref. 7] page 155 ff.]. This would be particularly true of mobile layers where, even though interaction forces are of short range, a high coverage density would insure many opportunities for encounter and repulsion.

To account for the behavior observed subsequent to annealing at a high temperature in an oxygen atmosphere, the following model is proposed. The annealing process creates a surface condition, possibly a structural change of some type, which admits a large oxygen chemisorption. Whether as 0_2 or as oxygen atoms is not apparent. The adsorbed species traps electrons from the conduction band, causing a higher resistance. As the temperature is raised from 300°K to 673°K. Some of chemisorbed species are lost from the surface, releasing electrons which are free again to move in the conduction band.

The shift to higher slopes at higher 0_2 partial pressures is accounted for by superimposing the increased repulsive potential at the higher coverage on the already lowered heat of adsorption to give an enhanced slope.

In connection with the possibility of change of structure upon annealing, Trapnell [Ref. 7, p. 142] cites work which has shown that different structural changes occur in manganese dioxide when heated in oxygen and the outgassed or in hydrogen and then outgassed or in CO

and then outgassed. These changes in structure are found to be different phases, i.e., regions with lattice structure of MnO, or Mn_2O_3 present in relative amounts depending upon the treatment. It is conceivable that similar changes could occur in zinc oxide.

Effects of gases other than oxygen. - When an un-annealed zinc film is cooled at a constant rate from 673°K to room temperature under ambient gases other than oxygen there is a difference noted in the magnitude and the slope of the log R versus 1/T curves, when compared to the curves for an oxygen ambient at the same pressure. Table 3 summarizes these results for the slopes in terms of activation energies, and plots of the data are shown in Figures 12 and 13.

TABLE 3

DEPENDENCE OF THERMAL ACTIVATION ENERGY ON TYPE OF GAS AND PRESSURE FOR 180 nm FILM

Pressure	Activation Energy (eV)		
(N/m^2)	Ar	N_2	O_2
13.3	0.155	0.124	0.254
133	0.112	0.094	0.310

The resistance levels of the films in Ar or N_2 do not significantly change with pressure whereas in O_2 the resistance changes by a factor of about 6 at 573°K to about 15 at room temperature.

This behavior can be interpreted by assuming that the adsorption behavior of oxygen on zinc oxide is different from that of Ar or N_2. Since argon is a noble gas with a completed valence shell it is most probably adsorbed to the ZnO surface by relatively weak, short range forces. Such physical adsorption, as distinguished from chemical adsorption characterized by electronic interaction and much higher (usually) adsorption energies is discussed by Trapnell [Ref. 7]. Since nitrogen gas has little influence on the electrical resistance of the film, it must also be physically adsorbed.

In contrast, oxygen must be chemically adsorbed and in so doing it influences significantly the electrical behavior of the zinc oxide. This is no new observation. The behavior has been reported by many workers [Ref. 1, 2, 9, 10]. The interaction between chemisorbed species and charge carriers in semiconductors has been examined in detail by Volkenstein [Ref. 11]. Present experimental data on sputtered ZnO films indicates that these are sensitive to oxygen, which is adsorbed to the

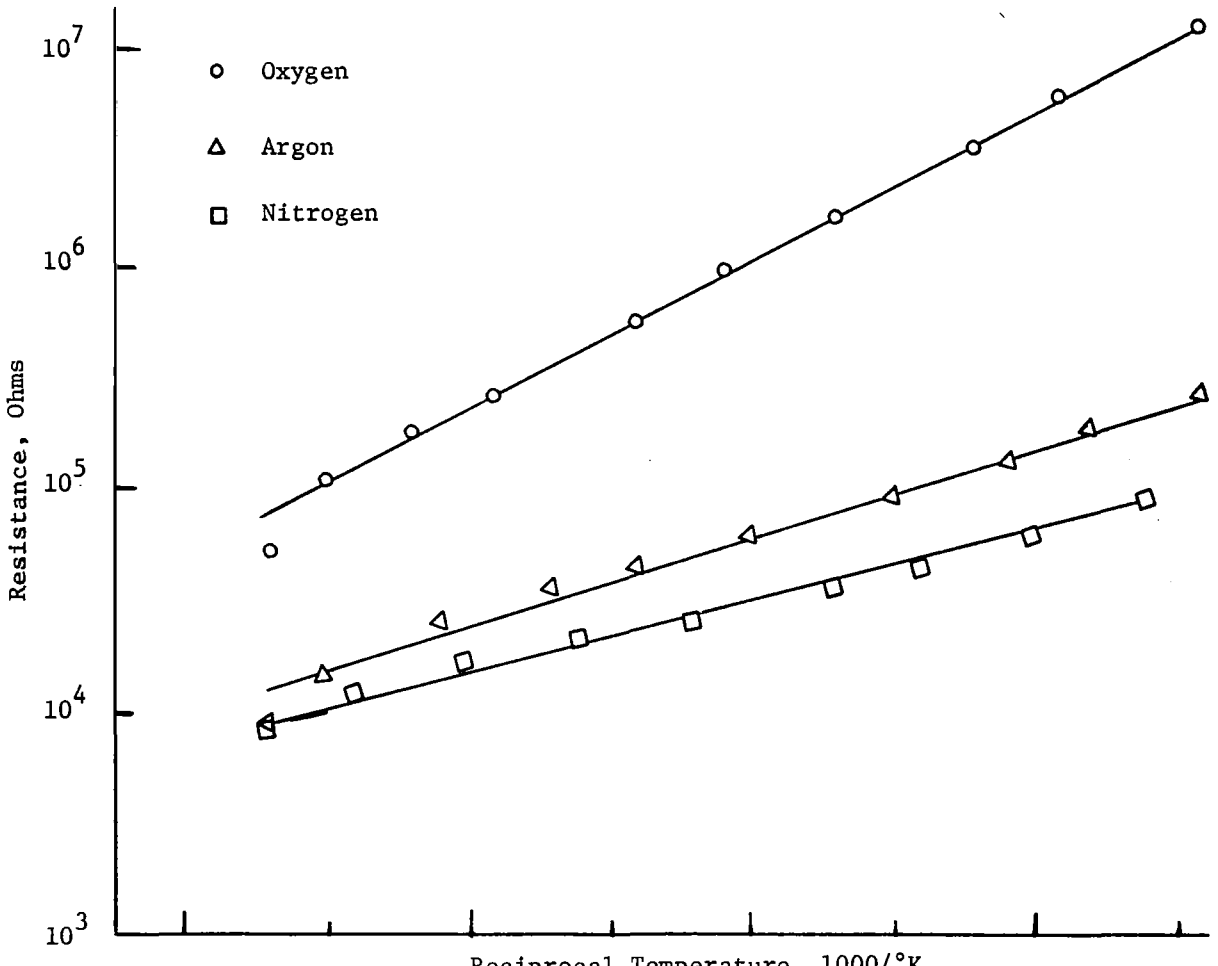

Figure 12. Resistance As a Function of Reciprocal Temperature for 180 nm ZnO Film Taken at a Constant Cooling Rate at a Pressure of 13.3 N/m^2 (0.1 torr) of the Gases Indicated.

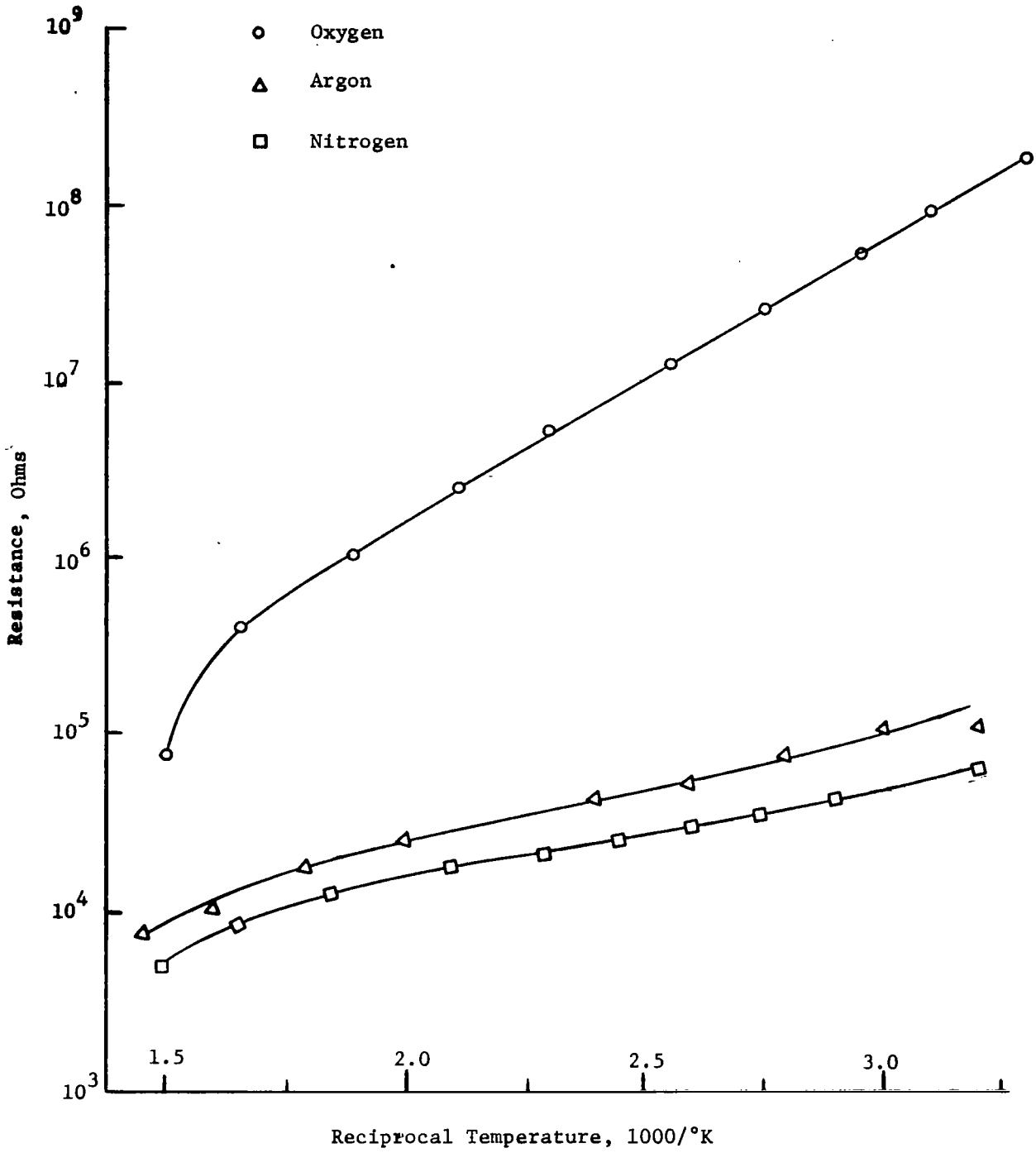

Figure 13. Resistance As a Function of Reciprocal Temperature for 180 nm ZnO Film at a Constant Cooling Rate at a Pressure of 133 N/m^2(1 torr) of the Gases Indicated.

surface by trapping an electron at the surface adjacent to the adsorbed species. Whether or not the adsorbate is O_2 or O is indeterminate from the data obtained in the present work.

Transient Response of Films. - The transient response of un-annealed ZnO films at a constant temperature and monitoring the film resistance as the ambient gas was again changed from pure nitrogen at a constant pressure to oxygen at the same pressure. After allowing time for the film resistance to stabilize at the new value, the gas ambient was again changed, back to the original N_2, and the resistance monitored. Results of these tests are shown in Figures 14, 15, 16, 17 and 18.

The 180 nm film was the most sensitive in terms of greater change of resistance and faster change of resistance as the gas ambient changed. The 360 nm was much less sensitive and has a much slower response. Response of the 90 nm film was not quite as sensitive as the 180 nm film, but was considerably more sensitive than the 360 nm film.

By comparing the response of the three film thicknesses at temperatures ranging from 638°K to 669°K it can be seen that increasing temperature speeds up the response. This can be interpreted on a kinetic basis using the conventional theory of adsorption, as discussed, for example by Trapnell [Ref. 7, Chapter 3]. In this theory the fraction of incoming gas molecules which stick to the surface depends upon the factor $\exp(-E_A/kT)$ where E_A is the adsorption activation energy and T is the temperature. The fraction of adsorbed molecules which escapes back into the gas phase is proportional to $\exp(-E_D/kT)$, where E_D is the activation energy for desorption. It can be seen that for activation energies, E_A and E_D, on the order of an eV or more, the adsorption and desorption rates will be sensitive functions of temperature.

The slower response time of the thick (360 nm) film compared to the other films may possibly be due to some permeability of the film to oxygen, with consequent mass transport by diffusion into and out of the film. This is examined in detail in Section III for the annealed films used as sensors.

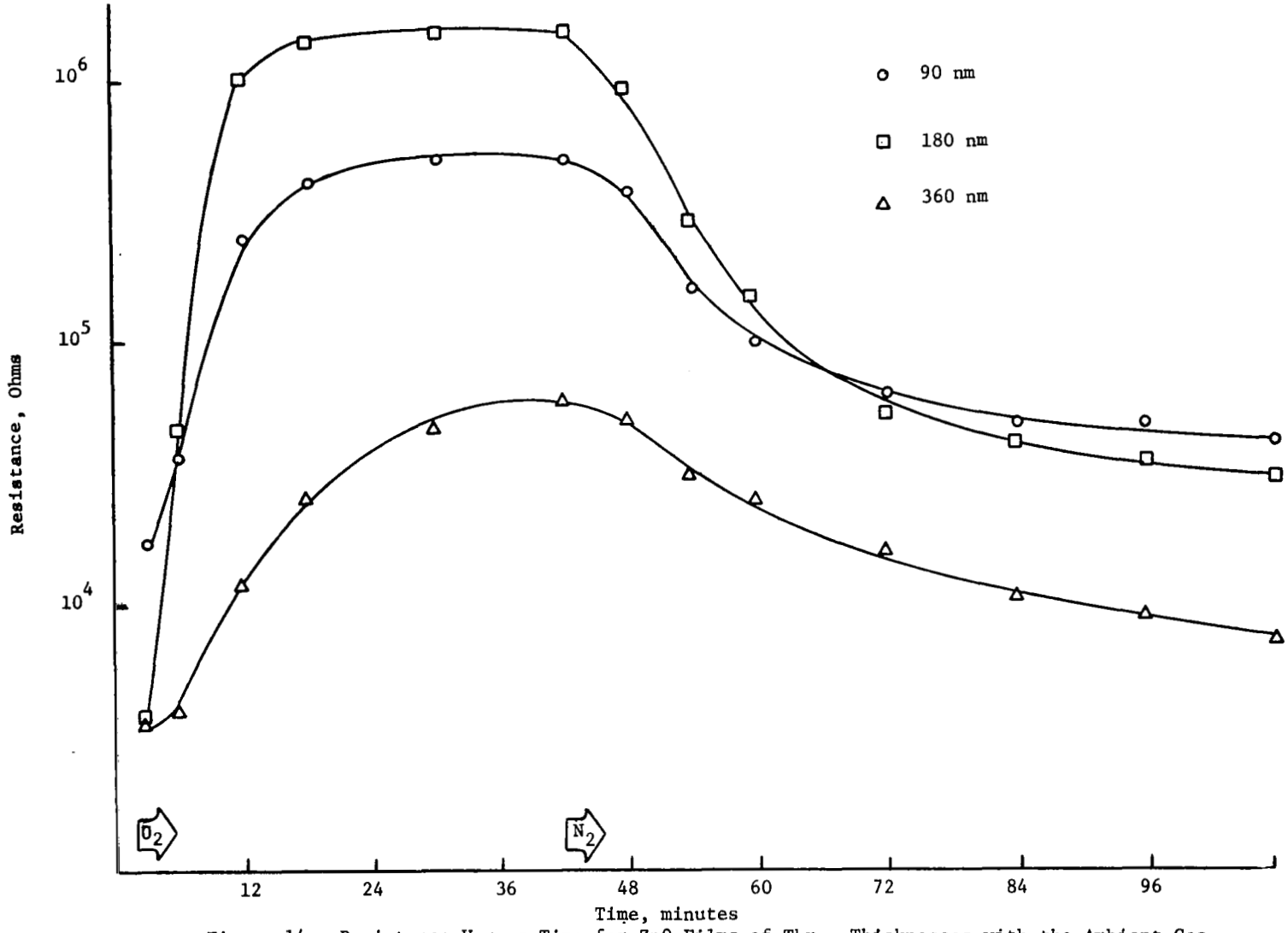

Figure 14. Resistance Versus Time for ZnO Films of Three Thicknesses with the Ambient Gas Switched from N_2 to O_2 and Back at 133 N/m^2(1 torr) Pressure. Film Temperature 638°K.

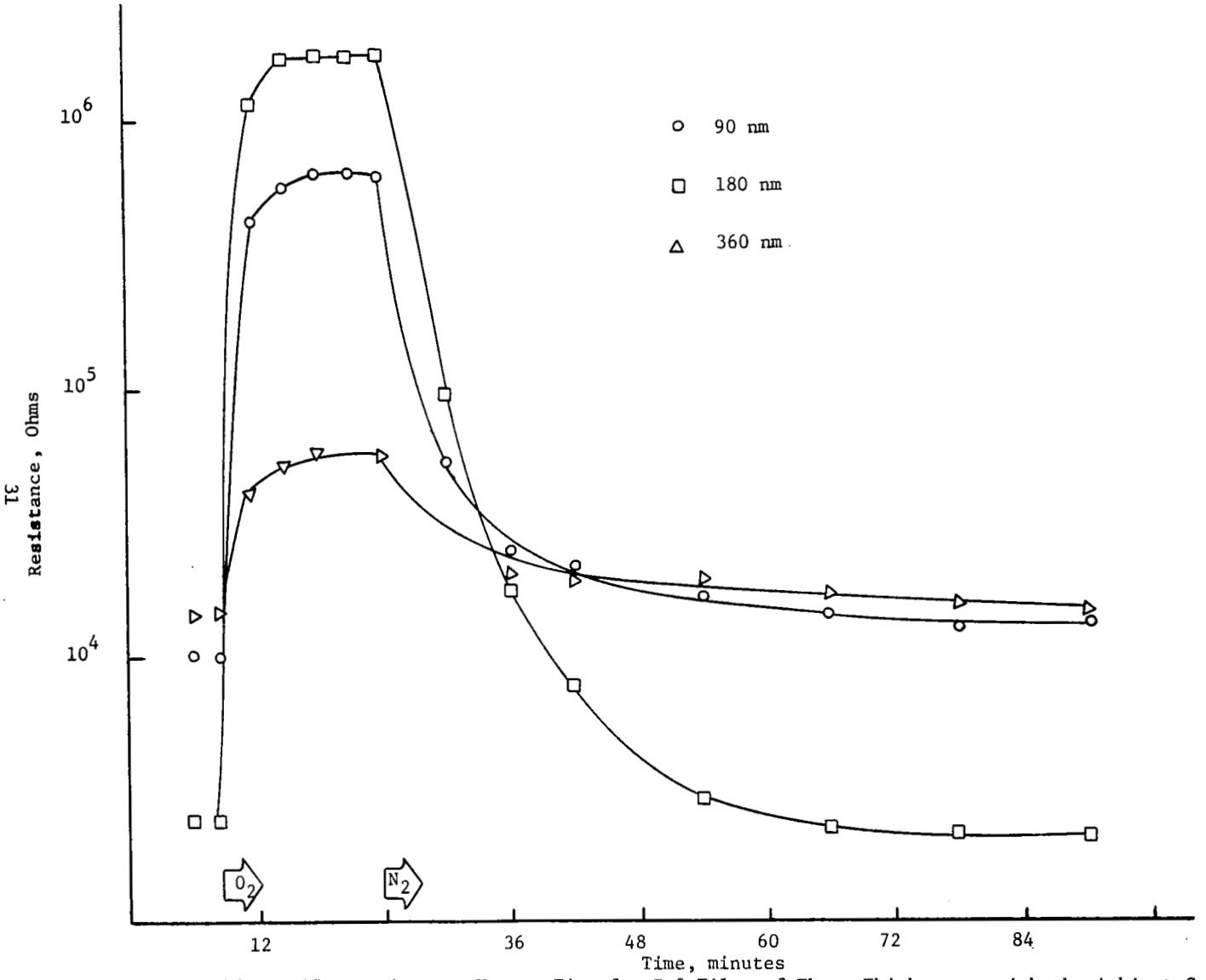

Figure 15. Resistance Versus Time for ZnO Films of Three Thicknesses with the Ambient Gas Switched from N_2 to O_2 and Back at 133 N/m^2(1 torr) Pressure. Film Temperature 650°K.

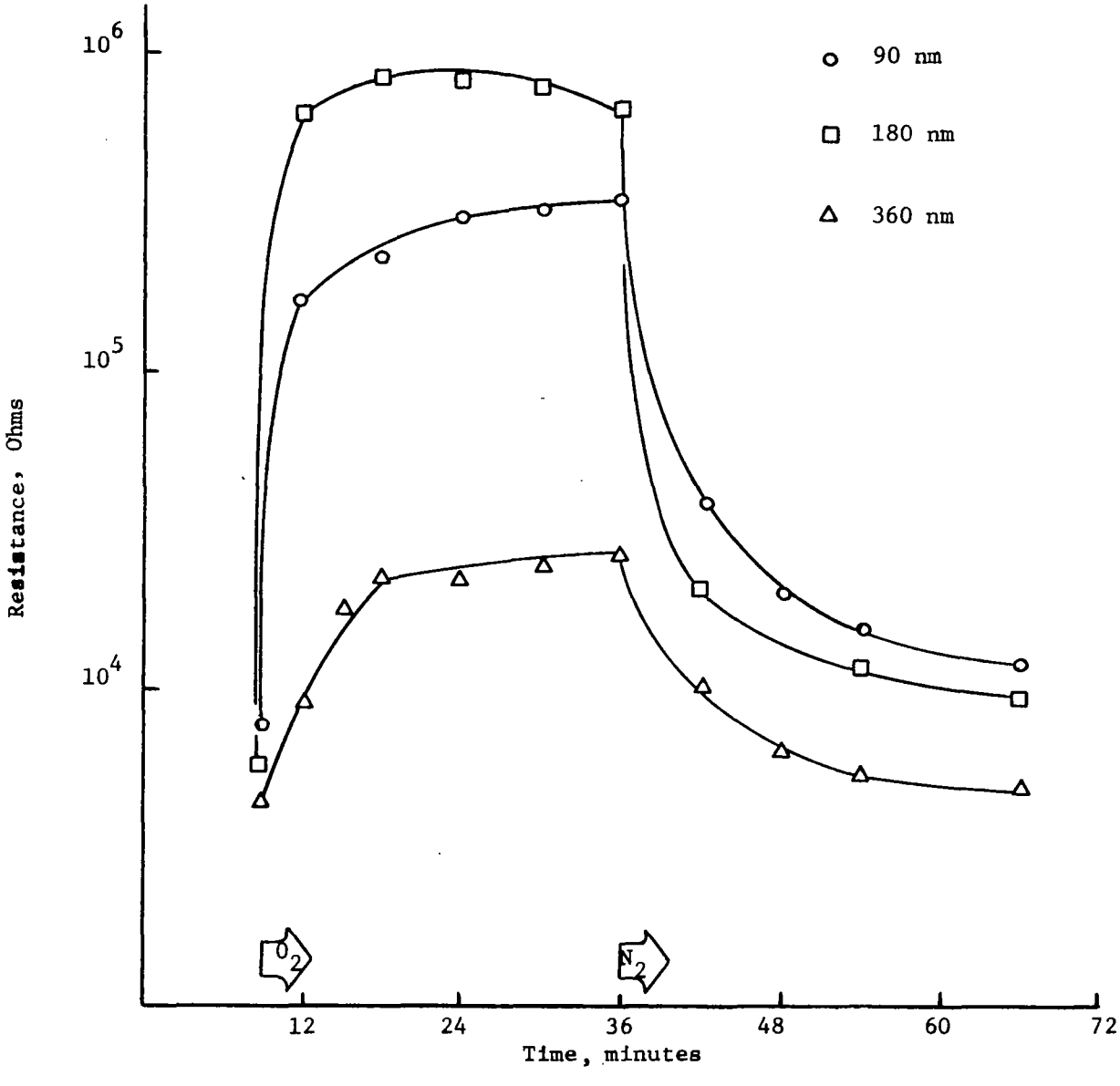

Figure 16. Resistance Versus Time for ZnO Films of Three Thicknesses with the Ambient Gas Switched from N_2 to O_2 and Back at 133 N/m^2 (1 torr) Pressure. Film Temperature 669°K.

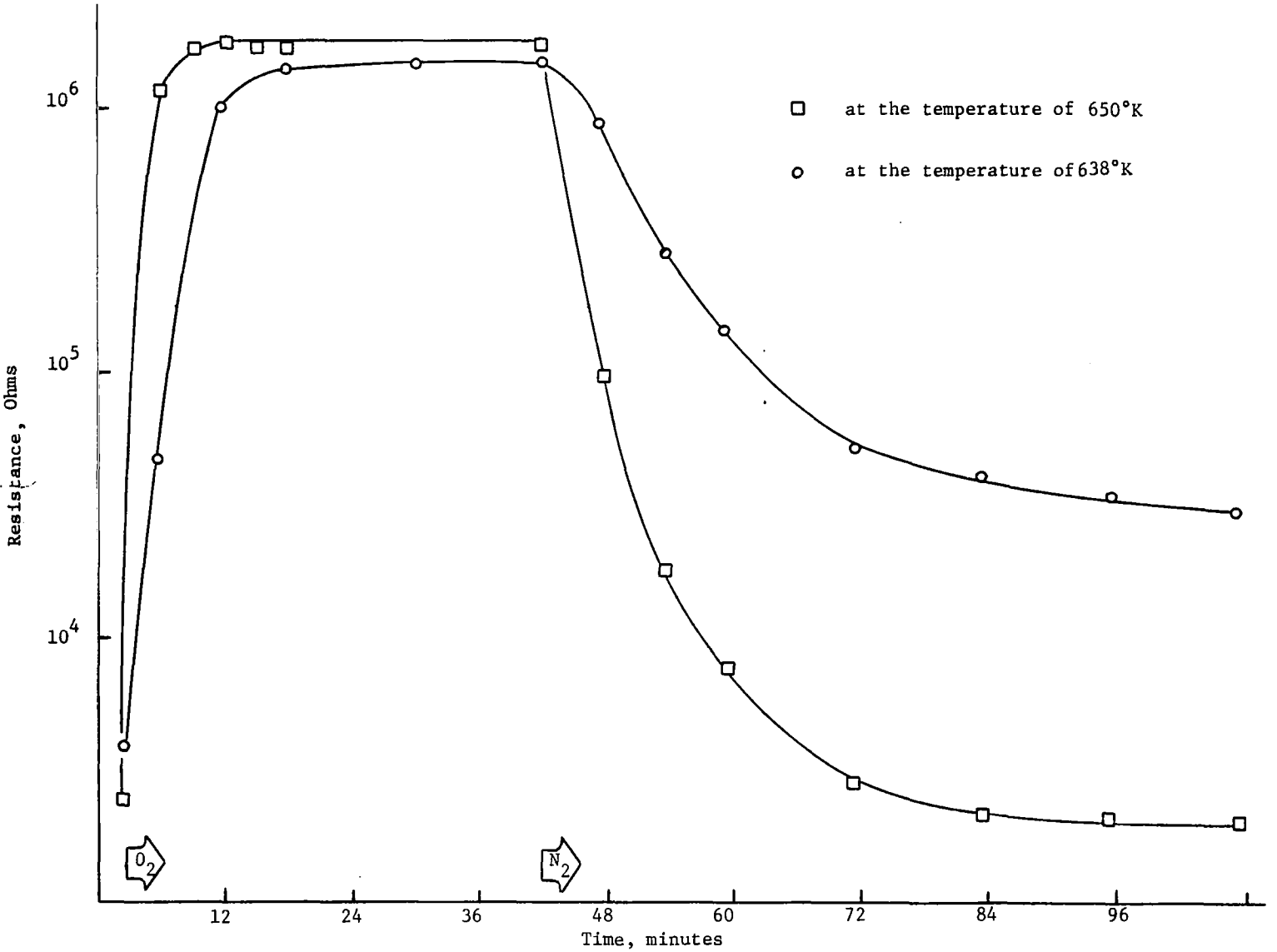

Figure 17. Resistance Versus Time for ZnO Film of 180 nm Thicknesses with Ambient Gases Switched from N_2 to O_2 and Back at 133 N/m^2(1 torr). Film at Temperatures Indicated.

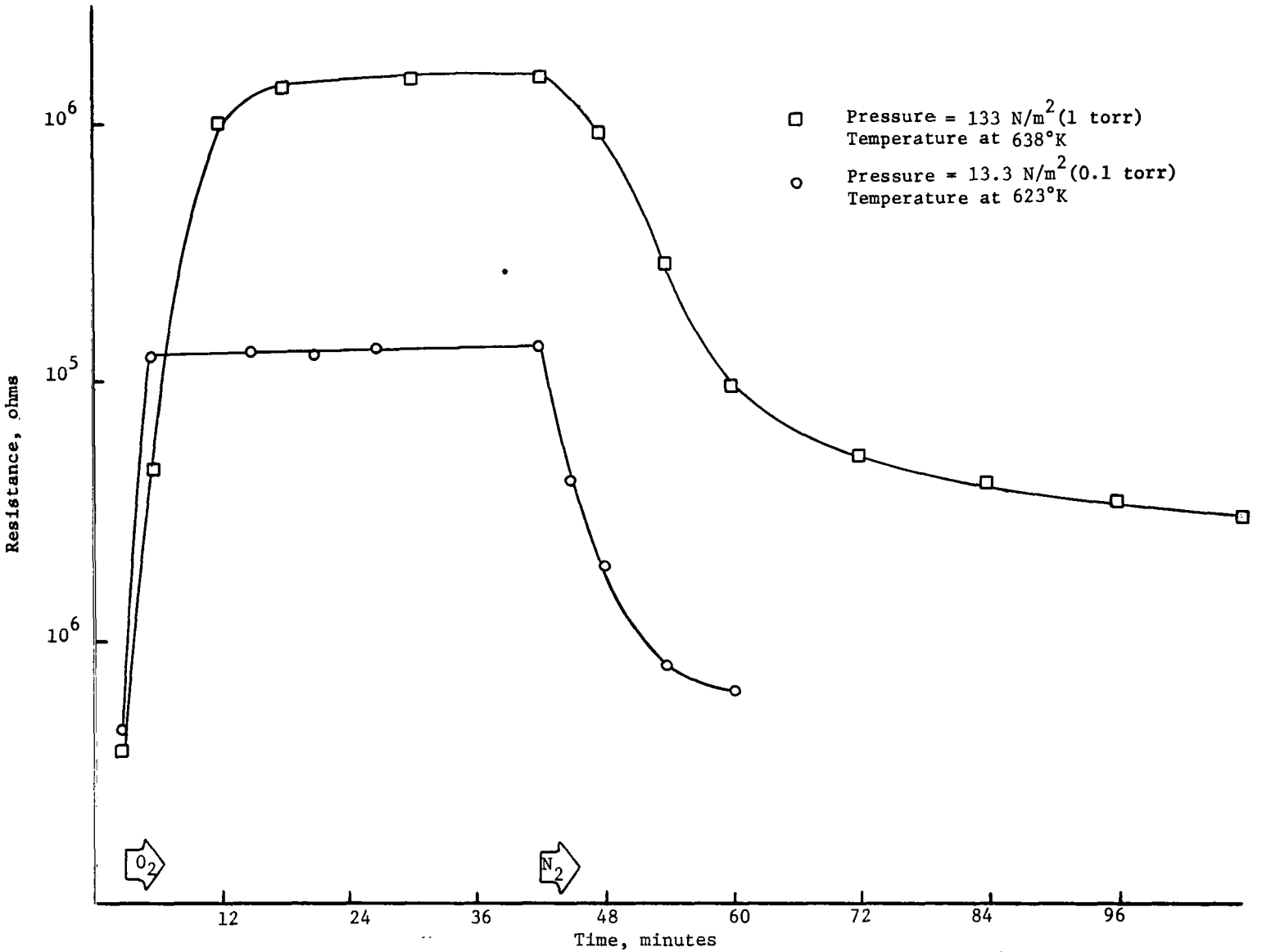

Figure 18. Resistance Versus Time for ZnO Film of 180 nm Thickness with Ambient Gas Switched from N_2 to O_2 and Back at the Pressure and Temperature Indicated.

SECTION III

SENSOR DESIGN, CONSTRUCTION AND CHARACTERISTICS

Design and Construction Features

In order to meet the requirements of space flight an oxygen partial pressure sensor must be of small size, low weight and have a low power consumption. All three of these requirements are compatible, but fabrication difficulty increases as the physical size decreases. This introduces a practical minimum size which may possibly be further reduced by technological improvement.

Previous work [Ref. 2] on ZnO films prepared by oxidizing evaporated layers of zinc had established that operation of these films at about 673°K provided a fairly rapid response and gave a small shift in resistance with temperature at constant O_2 partial pressure. The ZnO sensor of the cited work [Ref. 2] was heated by a wire wound heater which was inserted within a tubular substrate supporting the ZnO layer. The temperature of the heater was monitored for control purposes by a platinum resistance thermometer inserted within the tubular form which supported the heater wires.

Pearson [Ref. 4] proposed the use of a small semiconductor bar as a heater for a ZnO oxygen partial pressure sensor and demonstrated the feasibility of using silicon as the heater material. Furthermore, he proposed the use of the unique relation between resistance and temperature for silicon in the intrinsic range as a method of sensing and controlling the temperature.

The work reported below has achieved a workable miniature oxygen partial pressure sensor by combining the silicon heater/temperature sensor concept and reproducible sputtered thin films of ZnO. In describing how this was accomplished, and discussing the problems encountered in the reduction to practice, it is convenient to consider the development in several areas: the silicon heater and its contact problems, the insulating layer required between the low resistance silicon bar and the high resistance ZnO layer, the sputtered ZnO layer and its contacts, the sensor housing and the circuits for temperature control and signal conditioning.

Silicon Heater. - Silicon which has been doped to obtain extrinsic properties exhibits a unique resistance versus temperature relation for a given impurity concentration. Therefore, maintaining the temperature

at a constant value yield a constant resistance, and vice versa. This provides a method of monitoring the temperature of a specimen of Si and controlling it at a desired level. By the proper selection of impurity concentration, the resistance of a small bar of Si can be selected such that it will adequately heat a superimposed ZnO layer at the desired level of about 673°K with moderate values of supply voltage and current.

Pearson [Ref. 4] has estimated the resistivity range required for operating a silicon bar of about 1.27 cm length by 25.4 μm to .127 cm diameter at 673°K from a supply of less than 100 volts, drawing a current of up to 100 milliamperes, and finds a range of 0.002 to 100 ohm-centimeters is satisfactory. In the cited work experimental measurements were made on 0.8 ohm-cm Si bars, 1.27 cm long by 0.5 mm diameter with the center part .25 mm dia for 6.25 mm. With a power dissipation of about 2.5 watts, a temperature of 673°K was maintained at the center of the bar. Typically the temperature dropped off in a roughly parabolic manner toward the ends of the bar with a change of less than 50°K over the center 0.25 cm.

A similar geometry was used for the initial sensors constructed for this project. The silicon was covered by a thermally grown silicon dioxide layer of about 1 μm thickness and a ZnO layer sputtered onto the SiO_2. However, as will be subsequently described electrical leakage thru the oxide forced abandonment of the SiO_2 isolation layer. To provide a better insulation between the ZnO and Si a layer of a commercially available fusible glass cement was used. This will be described in detail later. This necessitated going to a larger cross section to minimize the problem of breakage during application of the ceramic layer.

The Si heaters used with the ceramic insulation were 1.27 to 1.59 cm long with a square cross section of 1 mm on a side. Initially 0.01 ohm-cm silicon was used but the current required to obtain a 673°K operating temperature was excessive. Use of nominal 4 ohm-cm silicon enabled attainment of the desired operating temperature with about 100 milliamperes of current and a voltage drop of 20 to 25 volts during operation. A much higher voltage, 80 to 100 volts, is required for the initial heat up of the bar since the resistivity at 300°K is much higher than at 673°K. A plot of resistance, voltage drop and current versus temperature for a typical heater bar is shown in Figure 19.

Establishment of reliable contacts on the silicon for heater leads was one of the problems encountered during the work. Pearson [Ref. 4] has discussed the problem of establishing ohmic contacts to a silicon bar operated at high temperatures. He reported that gold wires bonded to aluminum pads evaporated on the silicon bar melted at low values of current. He obtained reliable contacts by using fired-on liquid bright gold. Aluminum contacts were used initially in the present work and

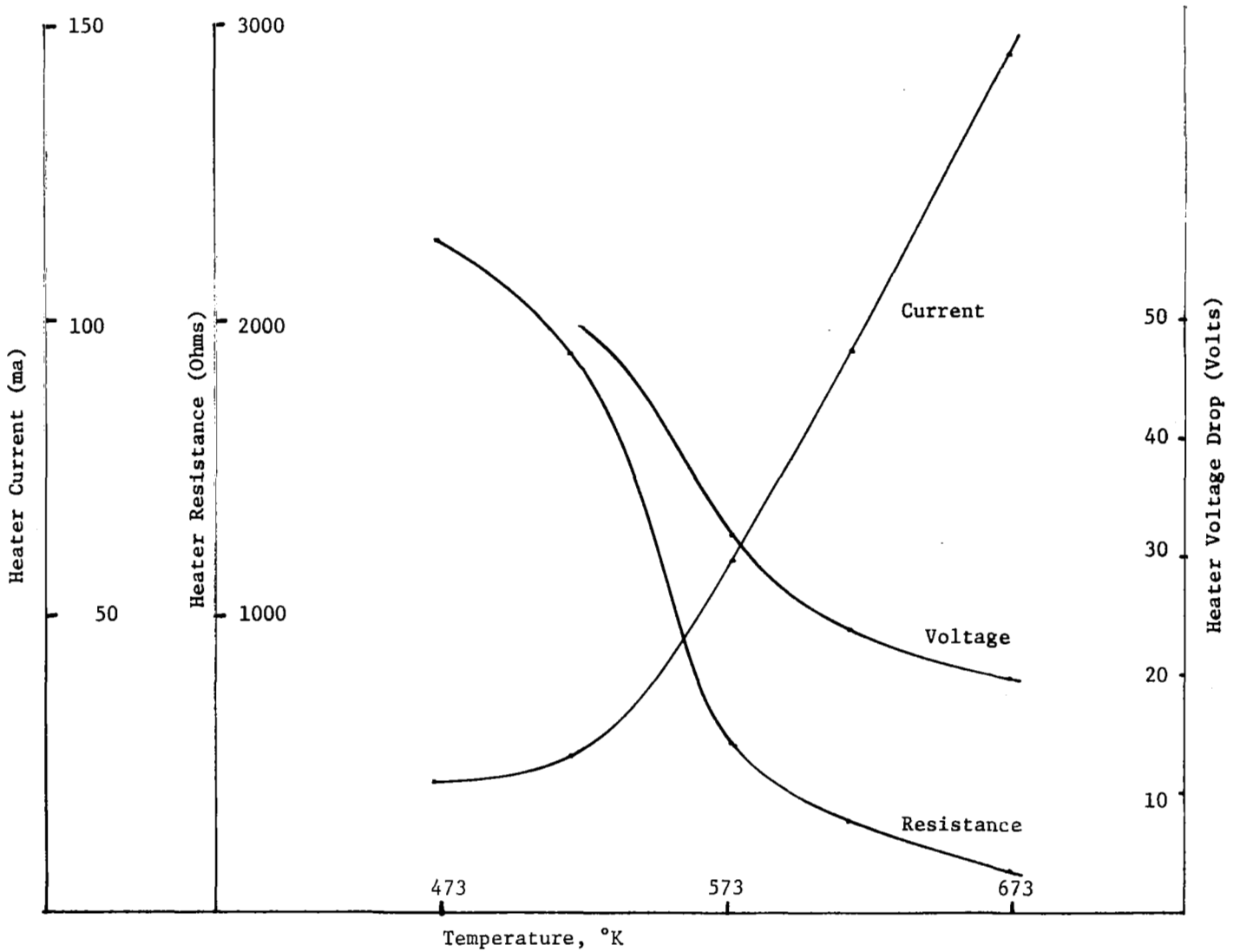

Figure 19. Voltage Drop, Current and Resistance Versus Temperature for a 4.0 ohm-cm, P-Type, Silicon Heater Bar.

appeared to operate satisfactorily, but since platinum was being used for contacts to the ZnO layers, it was also used for the heaters. Liquid bright platinum, fired at 673°K, gave almost linear current versus voltage characteristics on p-type silicon, but very non-linear characteristics on n-type silicon of the same resistivity (1 ohm-cm). Consequently, only p-type silicon was used for heater bars for the sensors. In operation, however, the platinum contact gold lead wire combination degraded. This problem was eliminated by evaporating a molybdenum layer over the fired-on Pt layer. Then a layer of liquid bright gold was applied over the molybdenum layer over the fired-on Pt layer. Then a layer of liquid bright gold was applied over the molybdenum and fired in subsequent operations when the ceramic insulation was cured at 1023°K and contacts were fired on the ZnO layer at 723°K. The Au/Mo/Pt combination yielded reliable contacts which were used for most of the measurements reported below.

Most of the measurements of the present work were carried out with a total gas flow rate of 100 cc/min, with the sensor mounted transverse to the flow in a pyrex tube of approximately 8 mm diameter as shown in Figure 20. This gave an average gas velocity of about 3.3 cm/sec. The effect of this flow on the power required to maintain a constant temperature is shown in Figure 21. Approximately 17.5 percent more power is required to maintain the temperature at 673°K when going from a no flow condition to a flow velocity on the order of 3.3 cm/sec. More significantly, at a constant power input of 2.3 watts the heater temperature can drop by about 40°K when going from a no flow condition to a flow velocity of about 3.3 cm/sec. This would give a decrease of resistance of the ZnO film which could be interpreted as a decrease in ambient O_2 partial pressure. To minimize this source of error, the heater should be controlled at a constant temperature, i.e., a constant resistance.

Insulating Layer. - The silicon heater provides a mechanical support for the oxygen sensitive ZnO layer, but a layer of insulation must intervene to electrically isolate the ZnO layer from the silicon bar. A layer of ZnO of the desired thickness is sputtered onto the insulating layer and ohmic contacts are made to the layer. Then leads are bonded to the ZnO contacts. A schematic of the arrangement is shown in Figure 22.

The isolating material should have a high electrical resistivity and a low thermal conductivity to minimize the temperature drop between the Si heater and the ZnO film. The thermal expansion coefficients of the three materials, Si, insulator and ZnO should match as closely as possible over the range of storage and operating temperatures expected, otherwise stresses caused by thermal cycling could possibly generate failure due to development of cracks which would change the resistance characteristics of the device with time.

The initial choice for an insulator was SiO_2. This was thermally grown to a thickness of about 1 μm. The ZnO was sputtered to the

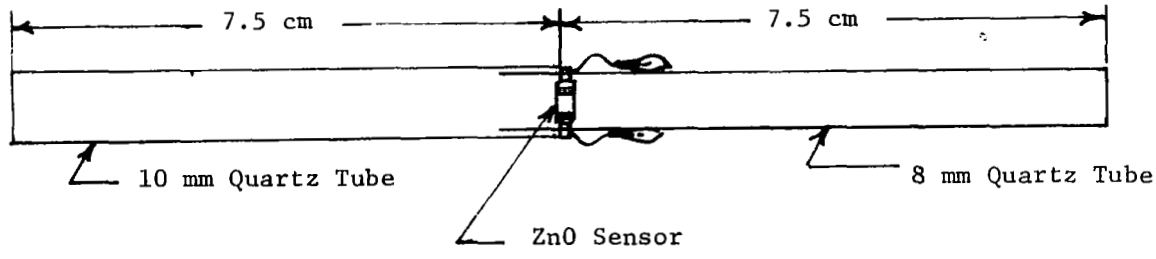

Figure 20. Arrangement of Sensor in Housing for Tests.

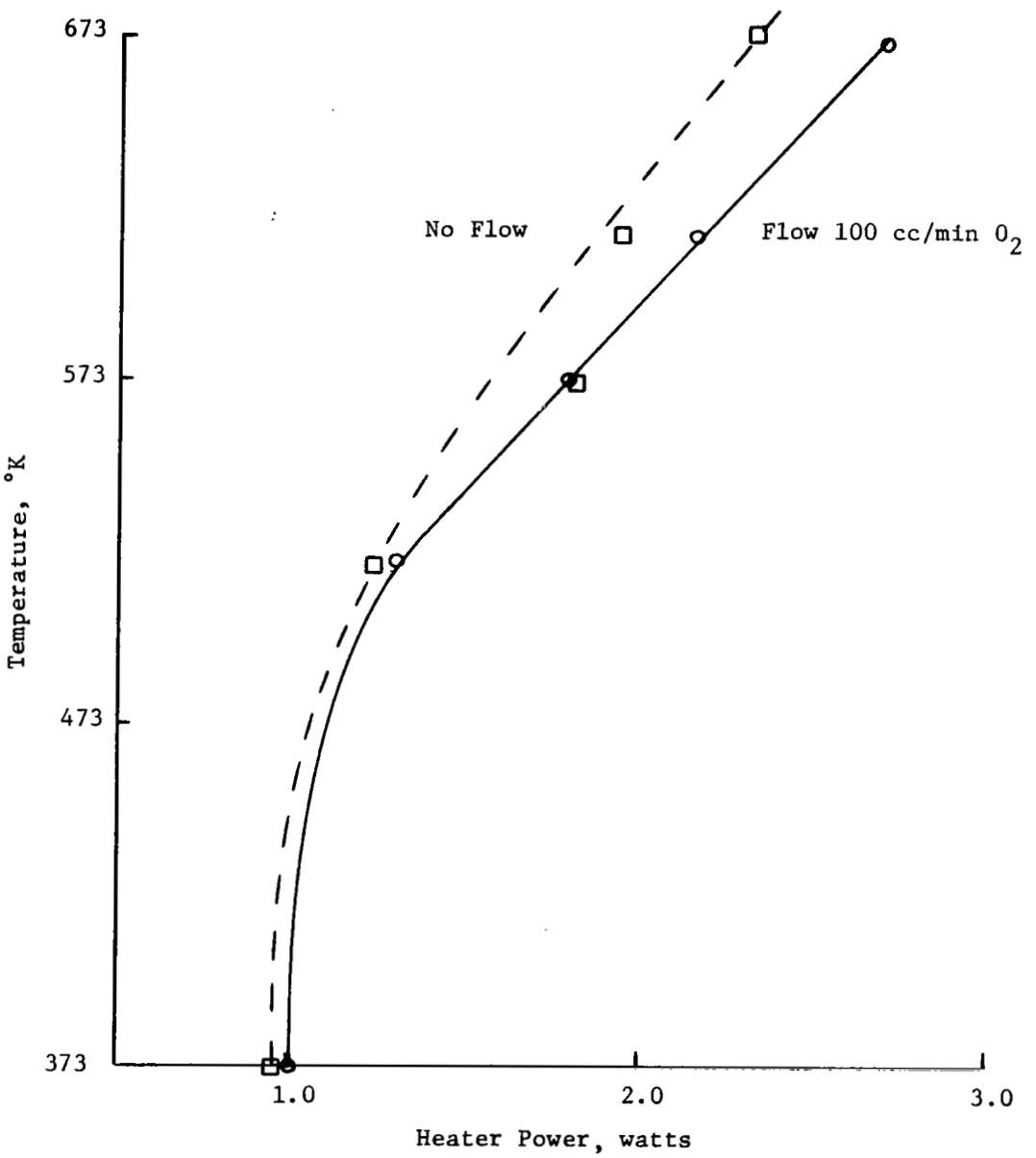

Figure 21. Heater Power Required to Maintain a Given Temperature Under Flow and No-Flow Conditions.

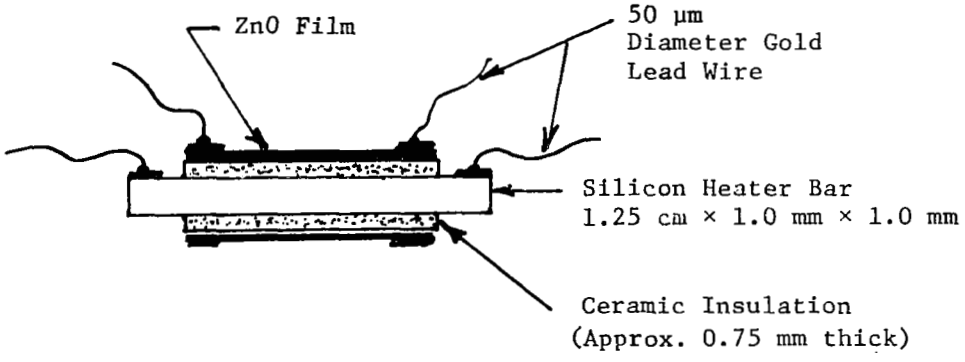

Figure 22. Section of Sensor Showing Construction.

desired thickness over the SiO_2. The center part of the ZnO layer for about 6.25 mm was covered with wax and the uncovered part of the ZnO etched off with acetic acid. Then wax was placed on the exposed SiO_2 layer to within about 5 mm of each end and the SiO_2 was etched off with hydrofluoric acid to expose contacting areas for the silicon. On this initial version of sensor, aluminum was evaporated onto the exposed Si ends to provide contacts for the heater leads. Platinum bands were painted on the borders of the ZnO region. After the platinum dried, gold wire was wrapped around these bands and another coat of liquid bright platinum applied. Then the sensor was baked at 673°K for one hour.

Sensors constructed in this manner exhibited a loss of sensitivity after several weeks operation at high temperature. This was attributed to degraded contacts and to leakage of the SiO_2 film. This leakage was evidenced by the presence of a d-c voltage across the ZnO film whenever a voltage was applied to the silicon heater bar. The leakage was attributed to "pin-holes" in the thermal oxide, a common problem [Ref. 12], but attempts to cover the "pin-holes" by deposited SiO_2 layers and sputterd Al_2O_3 layers over the thermally grown SiO_2 were not successful in alleviating the problem.

The SiO_2 insulation was abandoned and a layer of a commercially available fusible glass cement* was successfully used. This was applied as a powder suspension in a low viscosity liquid vehicle to the Si bars using a small brush. The suspension was then fired at 1023°K. The resulting insulating layer did not develop the leakage problem that had plagued the SiO_2 insulation. Tests at 673°K on a typical structure gave leakage resistance of over 1×10^7 ohms.

Zinc Oxide Layer. - Zinc oxide layers of various thicknesses, ranging from about 90 nm to about 360 nm were sputtered on the insulating layer. The ZnO layer in the center was covered with wax and ZnO was etched back from the ends to avoid any leakage paths to the silicon heater bar. Platinum contact bands were made on the zinc oxide by painting on liquid bright platinum and firing at 673°K to 723°K. Initially leads were bonded by wrapping gold wire around the Pt bands and coating these with another layer of liquid bright platinum, which was then fired. This method was abandoned in favor of the simpler procedure of bonding on 50 μm dia gold wires with a thermocompression ball bonder. However, contacts made by this method degraded with time at high temperature. This was attributed to the gold ball punching through the Pt layer to make direct contact with the ZnO layer. Previous experience had shown that a ZnO/Au contact was subject

*Corning Glass Works Brand "Pyroceram."

to deterioration at high temperature. This problem was avoided by extending the Pt bands beyond the edge of the ZnO layer onto the ceramic. Then the gold leads were bonded to the Pt over the ceramic. This method provided reliable high temperature contacts.

The resulting structure typically exposed a band of about 2.5 mm to about 3 mm width of active ZnO at the center of the bar. This band was covered over most of the perimeter with zinc oxide. The ZnO was activated prior to bonding on the gold leads by placing the sensor in an oven and heating to 873°K in ambient air, and then cooling slowly from 873°K back to room temperature in ambient air. Following the activation annealing gold lead wires were bonded to the platinum contacts to the ZnO and to Au/Mo/Pt contacts on the silicon heater bar.

Sensor Housing. - Initial tests were carried out with the sensing elements simply laying on a glass substrate and inserting into a quartz tube as shown in Figure 23. Response times were not as fast as expected nor was the sensitivity as good as expected. An anlaysis of the problem indicated that at the low input gas flow rates used, 100 cc/min total, the vessel volume to throughput ratio, V/Q, gave a large time constant. The problem was further aggravated by the fact that at the flow rates used, flow was laminar. This impeded mixing of the incoming and ambient gas. In addition the large diameter open end tube allowed considerable back diffusion O_2 at low O_2 input levels.

Consequently, the sensor was mounted transverse to the incoming gas flow lines in a 8 mm I.D. pyrex tube with the ends secured by epoxy cement in notches cut into the glass tube. Another tube of 10 mm I.D. was slipped over the end of the first tube adjacent to the sensor and cemented in place. Both tubes extended for three inches on either side of the sample. The exterior surface of the tubes was sprayed with black paint to minimize photoconductive effects in the zinc oxide. The gold leads from the sensor were connected to the external circuits by means of small copper wires taped to the pyrex tube to prevent any strain on the gold lead wires. For the introduction of test gas mixtures to the sensor, flexible tubing was placed over the smaller diameter glass tubing of the housing.

In this configuration the "hold-up" volume of the upstream side of sensor was about 4 cubic centimeters. At a flow rate of 100 cc/min, assuming perfect mixing, the time constant for this "hold-up" volume was about 2.5 seconds, which was not significant compared to the response times of the ZnO films.

Circuits for Temperature Control and Signal Conditioning. - As pointed out by Pearson [Ref. 4, page 19] the temperature of the silicon heater can be maintained constant by maintaining a constant resistance. Pearson suggested the use of a logarithmic ratio circuit for this purpose. Two other approaches were used in the experiments conducted on this aspect of the work. The first was a simple bridge circuit, shown

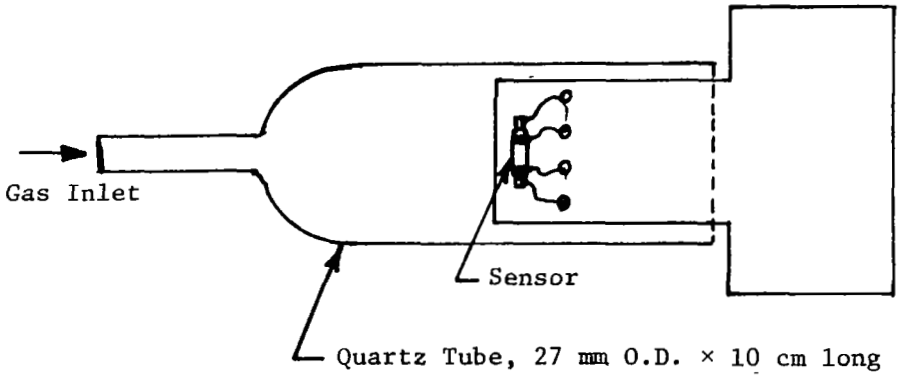

Figure 23. Sensor Arrangement Used for Initial Tests.

schematically in Figure 24. The second was a commercially available multiplier/divider analog circuit, which was connected as shown in Figure 25.

In the bridge type control circuit. The set point resistance R_S was selected to provide the desired heater resistance at the operating temperature. This heater resistance, R_H, was typically about 240 ohms, i.e. about 24 volts drop at 100 milliamperes. An increase of resistance due to cooling would increase the forward bias on Q2, providing more current drive to Q1 to raise the temperature of the heater. An opposite action occurs when the heater temperature rises and decreases the resistance of the silicon bar. The Zener diode is used to assure that the collector-emitter voltage rating of the transistor Q2 will not be exceeded.

The bridge circuit was tried initially without the large capacitor between the base and collector of transistor Q2. The circuit oscillated in this condition due to the relatively long lag time of the heater and the large loop gain through the feedback connection of Q2. Addition of the large capacitor, connected in the Miller integrator manner, showed the response of the control loop sufficiently to bring the current through the silicon heater bar smoothly up to the set point value, usually 100 milliamperes.

The circuit was tested over a period of several weeks and a random drift of about $\pm$ 5 milliamperes ($\pm$ 5% of set point current) maximum was noted. No effort was made to locate the source of the drift because a circuit employing a commercial circuit for multiplier/divider operation was available by this time and when put into operation proved to have much more stable characteristics. However, the bridge circuit should not be overlooked in any future design consideration. It is relatively simple, and most important, it can operate from the same voltage source that powers the heater.

The divider circuit selected as the heater control for the present design was a commercially available analog Multiplier/Divider connected to obtain an output voltage which is 10 times the ratio of the input voltages X/Y. The X input is proportional to the heater current. A bias resistor, R_B in Figure 25, is used to provide about 90% of the current drive required for Q1 to maintain about 100 milliamperes through the silicon heater bar. The controlling trim for temperature stability comes from the analog divider network monitoring the heater resistance.

The conductance of the ZnO layer is a strong function of oxygen partial pressure. A typical example of the ZnO film conductance versus oxygen partial pressure curve is given in Figure 26. Approximately 80% of the total

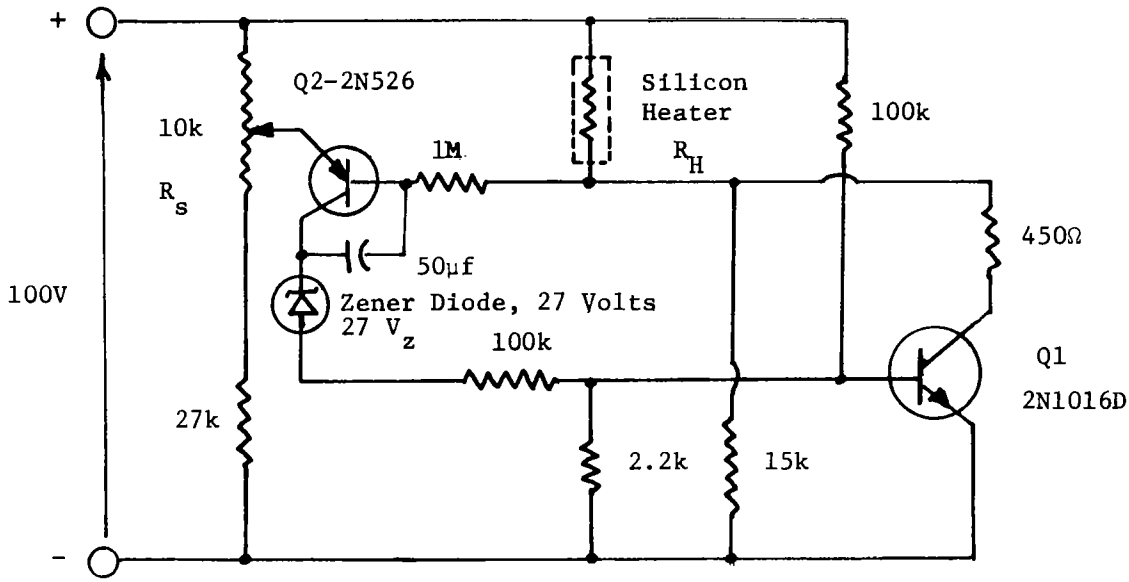

Figure 24. Circuit Diagram of Bridge Circuit Used to Control Silicon Heater Resistance.

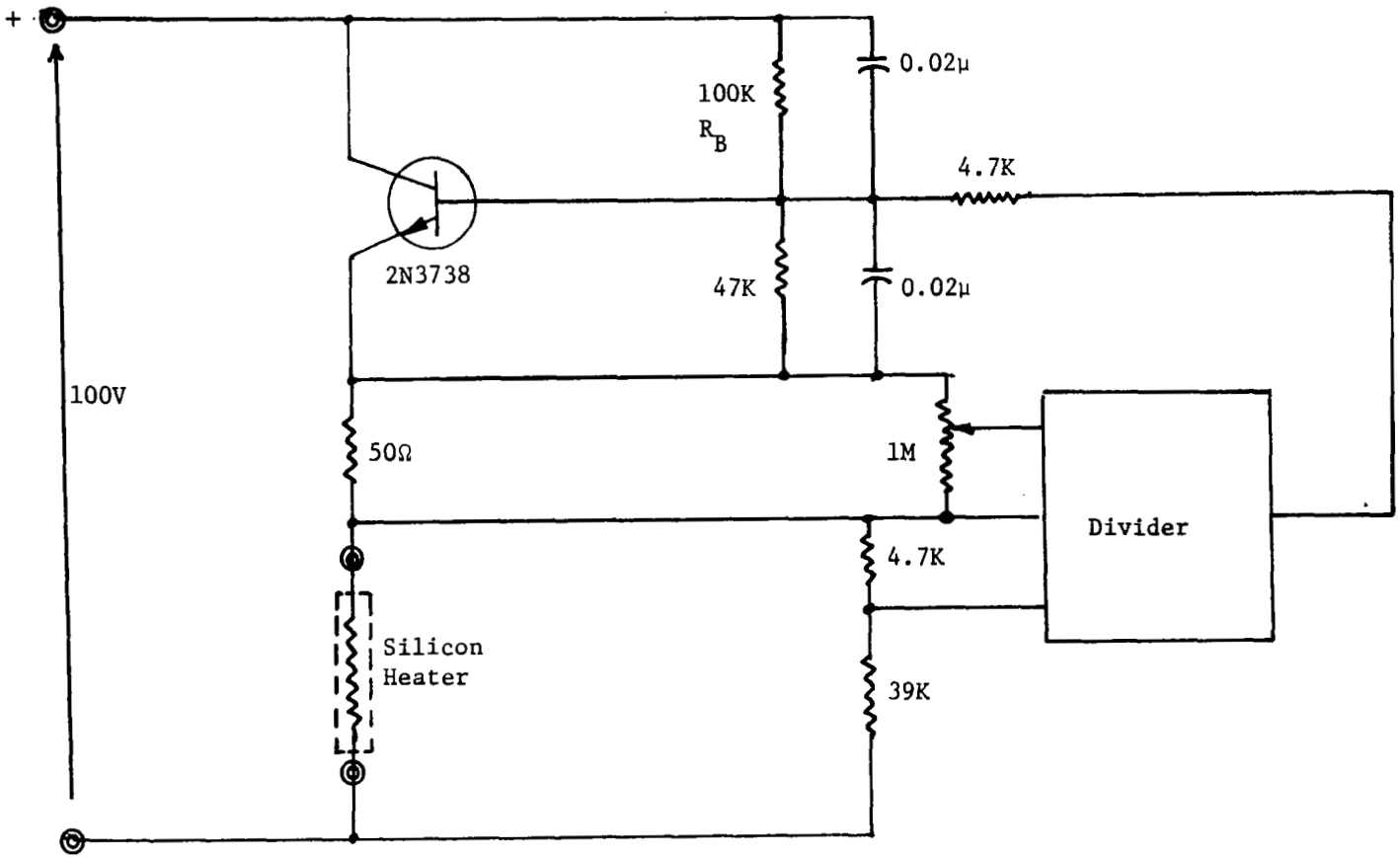

Figure 25. Schematic Diagram of Heater Controller Using Divider Network

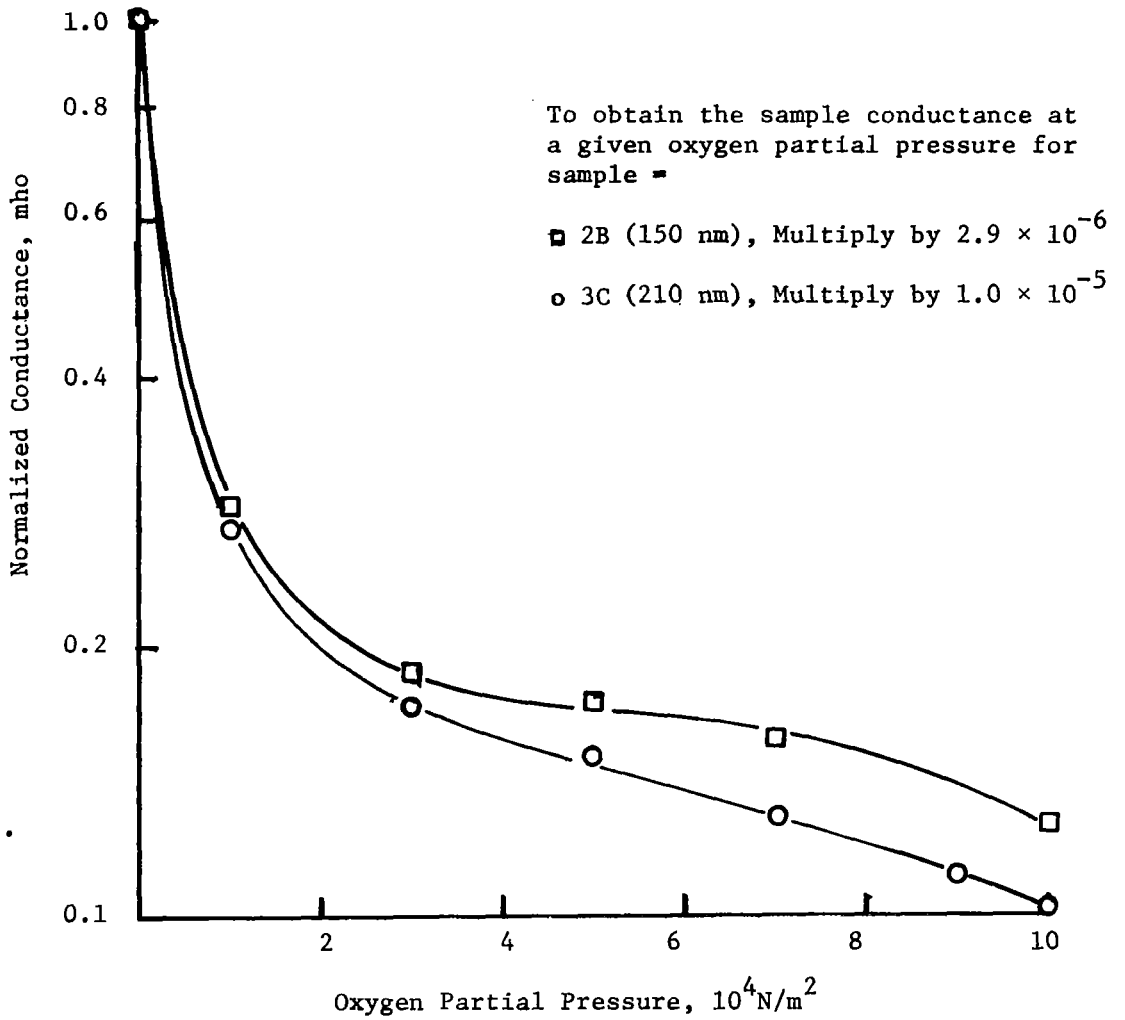

Figure 26. Conductance Versus Oxygen Partial Pressure for Two Sensor Samples.

change in conductance between 0_2 and $1 \times 10^5 N/m^2$ (760 torr) of 0_2 occurs between 0 N/m^2 and $2 \times 10^4 N/m^2$ (150 torr) or 20% of the total partial pressure range. For control and indication purposes it is desirable to linearize the signal as much as possible. This was accomplished by using operational amplifier circuits with non-linear elements in the feedback and coupling circuits to compensate for the non-linearity of the oxygen partial pressure response.

A simplified diagram of the signal conditioning circuit is given in Figure 27. Compression is achieved in the first stage by using a "trans-diode" connected transistor to obtain a logarithmic response. Through the use of a bias source and a variable resistance, the "zero" control, the output of Stage 2 is reduced to zero with 100% N_2(0 torr 0_2) flowing over the sensor. Gain of Stage 2 is variable by means of the variable resistor in the feedback loop. This provides a span adjustment to allow for variations in the conductance range for various sensors, improving interchangeability.

A typical example of the response of Stage 1 and Stage 2 combined with one of the sensor samples, number 3C, is shown in Figure 28. The voltage gain of Stage 2 was set at about 30 and the bias to Stage 2 adjusted to give zero volts with the sensor in 100% N_2 at 100 cc/min. Then the 0_2 content of the gas stream was increased in stages and the output voltage of the circuit measured. The logarithmic circuit provides the compression desired and give a faithful representation of the curve of Figure 26. For reduction of the response to a straight line, a non-linear gain is required which attenuates the lower range of the response curve and amplifies the upper range. This is accomplished by Stage 3.

In Stage 3, the gain of the amplifier is controlled in a non-linear manner by using a diode as part of the input resistance. The diode resistance decreases approximately exponentially as the current is increased. Therefore, the amplifier gain is low as small values of input and increases at the input increases. The shape of the gain versus input curve depends upon the relative sizes of the feedback resistor R_f, the diode resistance and the series and shunt input resistors, R_1 and R_2. Some control of the shape is obtained by making the shunt resistor, R_2, variable

A complete circuit diagram of the heater controller and signal conditioning circuits is given in Figure 29.

Sensor Properties

Response to Oxygen. - For evaluation of the response of the ZnO oxygen partial pressure sensor to oxygen, the experimental arrangement

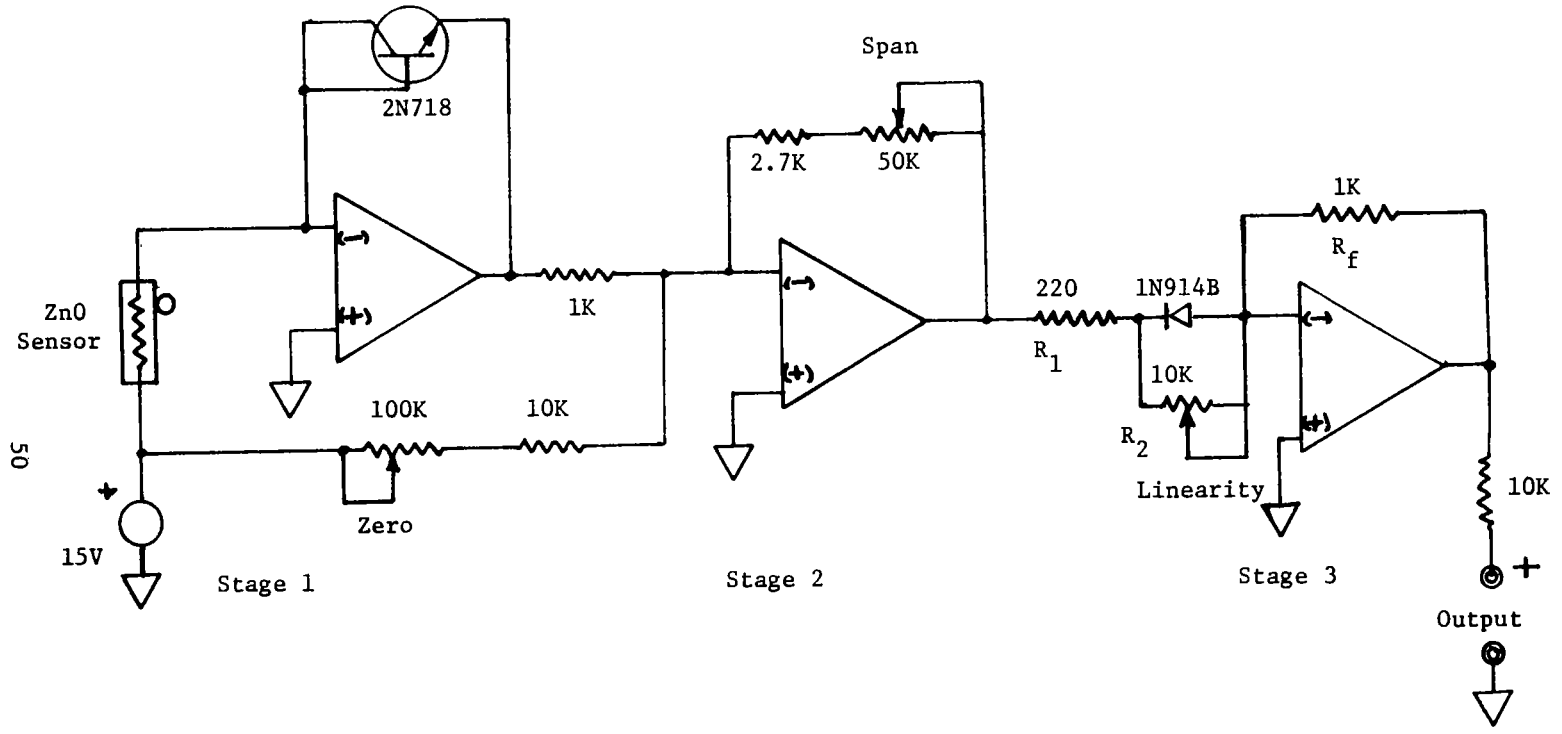

Figure 27. Signal Conditioning Circuit

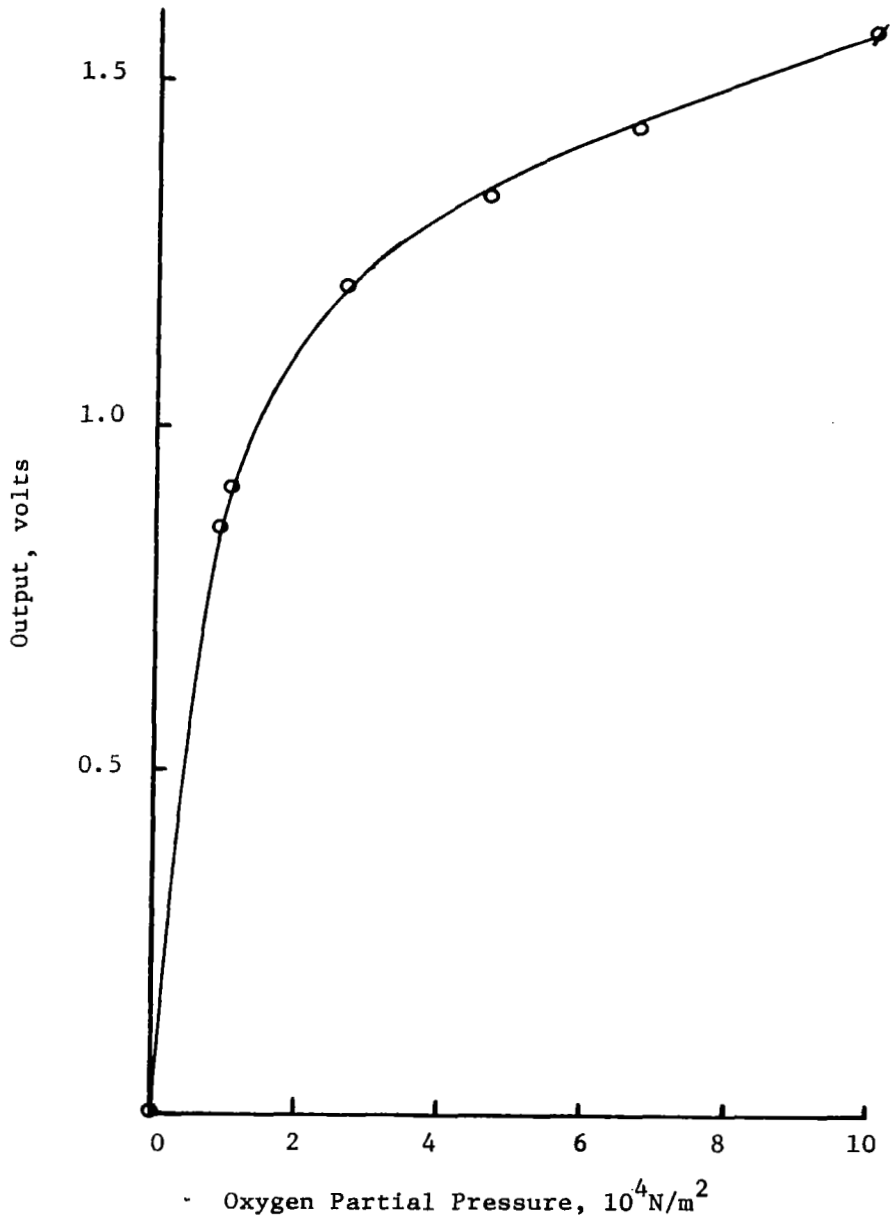

Figure 28. Output Voltage of Stage 2 with Sensor 3C in a Gas Stream of Variable Oxygen Partial Pressure.

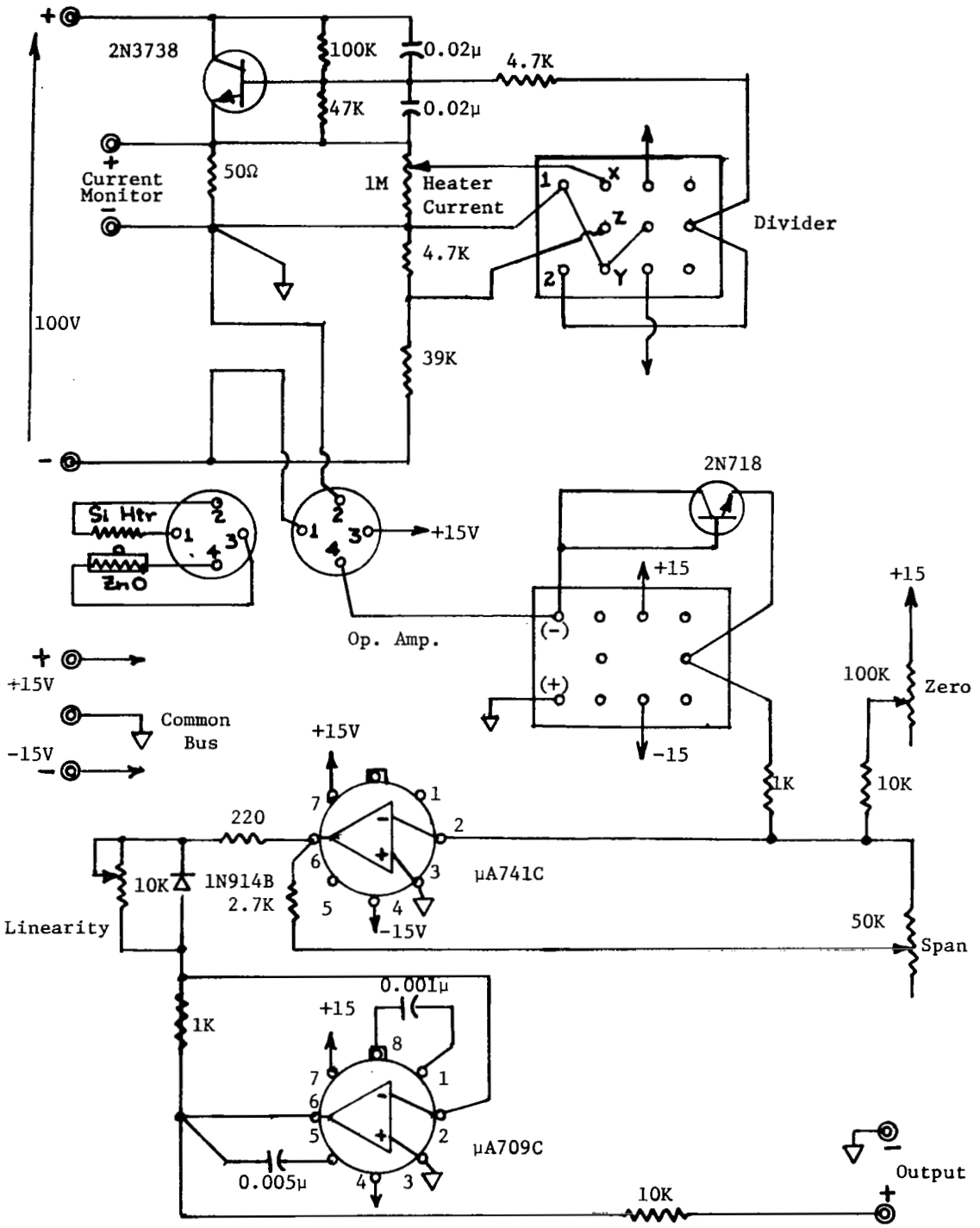

Figure 29. Complete Circuit Diagram

in Figure 30 was used. Metering valves MV3 and MV4 were set to give a 10% 0_2 stream controlled by shut off valve SV2. Metering valves MV1 and MV2 were used to vary the 0_2 percentage levels used in step and calibration tests. The power supply was set to operate the sensor at about 673°K with a gas flow rate of 100 cc/min. Initially the input line to the sensor was switched back and forth from 100% N_2 to 100% 0_2, allowing time for stabilization, to obtain the sensitivity

$$\frac{\Delta G}{G(0)} = \frac{G(0) - G(100)}{G(0)} \tag{16}$$

where G(0) is the conductance at zero oxygen, with 100 cc/min of N_2 at 760 torr flowing past the sensor, and G(100) is the conductance at 100% oxygen, 100 cc/min at $10^5 N/m^2$. The value found for $\Delta G/G(0)$ was approximately 0.9 for each of the sensors, regardless of thickness.

Then Line A in Figure 30 was set to maintain an oxygen partial pressure of about $10^4 N/m^2$ (76 torr) and the flow control values in Line B were adjusted to give partial pressue of oxygen from about 3×10^4 to about $9 \times 10^4 N/m^2$. Flow to the sensor was switched from Line A to Line B and vice versa, allowing time to stabilize in each case. In this manner the transient response and static response curve for each sensor was obtained.

The transient response times, given as the time required to go from 10% to 90% of the total change, for several sensors are given in Table 4. An interesting feature of the step response behavior, as can be seen from the data in the table, is that the desorption step for 0_2 is generally faster than the adsorption step. This behavior is consistent with the fact that the ZnO surface is much hotter than the gas ambient. A plot of resistance versus time for a 90 nm film responding to two different 0_2 partial pressure step increases is shown in Figure 31.

Another feature of the data is the increase in response time with relative thickness. This is shown in Figure 32. Also shown in the Figure is the curve obtained by taking

$$T_r = 30(\theta_r)^{7/2} \tag{17}$$

where T_r is the response time in minutes and θ_r the relative thickness

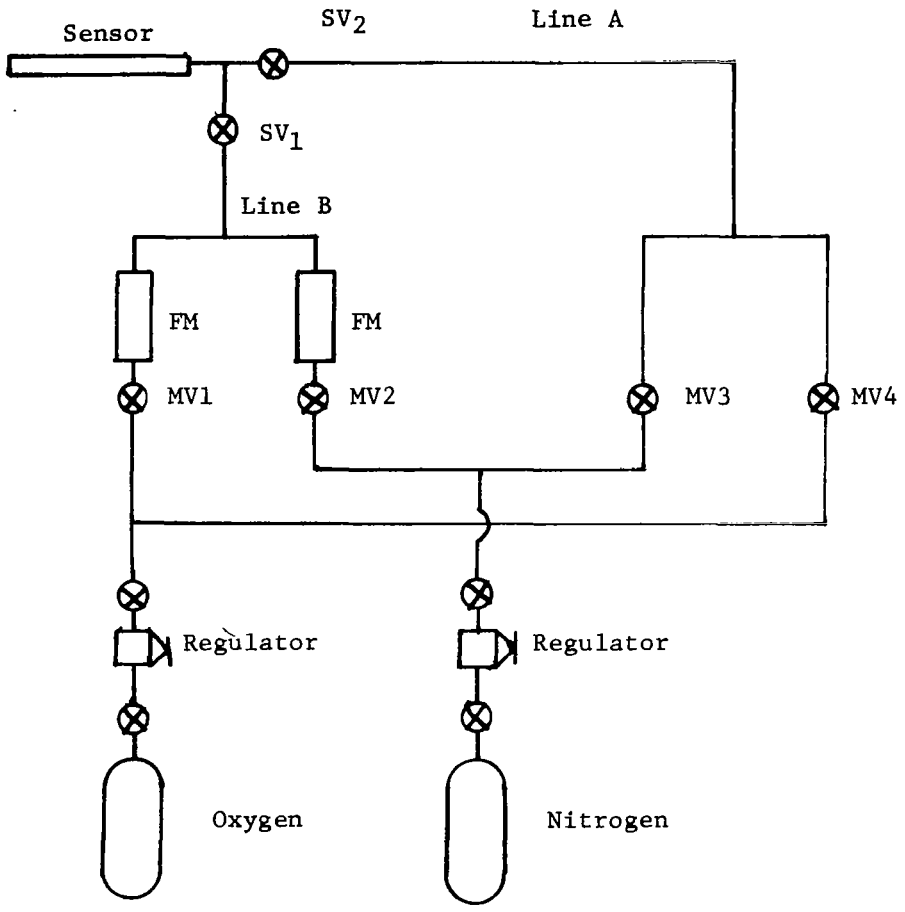

Figure 30. Flow Arrangement for Step Testing and Oxygen Calibration of Sensors.

Table 4. Step Response Times (10%-90% of Total Change) for Three ZnO Films

Step Size $10^4 N/m^2$	Direction	Response Time (Min.)
	Sample 4D 300 nm Thick	
8	incr O_2	24.4
6	decr O_2	11.3
6	incr O_2	17.5
4	decr O_2	10.6
4	incr O_2	17.5
2	decr O_2	14.7
2	incr O_2	6.87
	Sample 3C 210 nm Thick	
8	decr O_2	3.1
8	incr O_2	5.9
6	decr O_2	5.3
6	incr O_2	5.9
4	decr O_2	4.5
4	incr O_2	4.4
2	decr O_2	9.1
2	incr O_2	15.9
	Sample 1A 90 nm Thick	
6	incr O_2	0.47
6	decr O_2	0.19
4	incr O_2	0.38
4	decr O_2	0.19
2	incr O_2	0.31

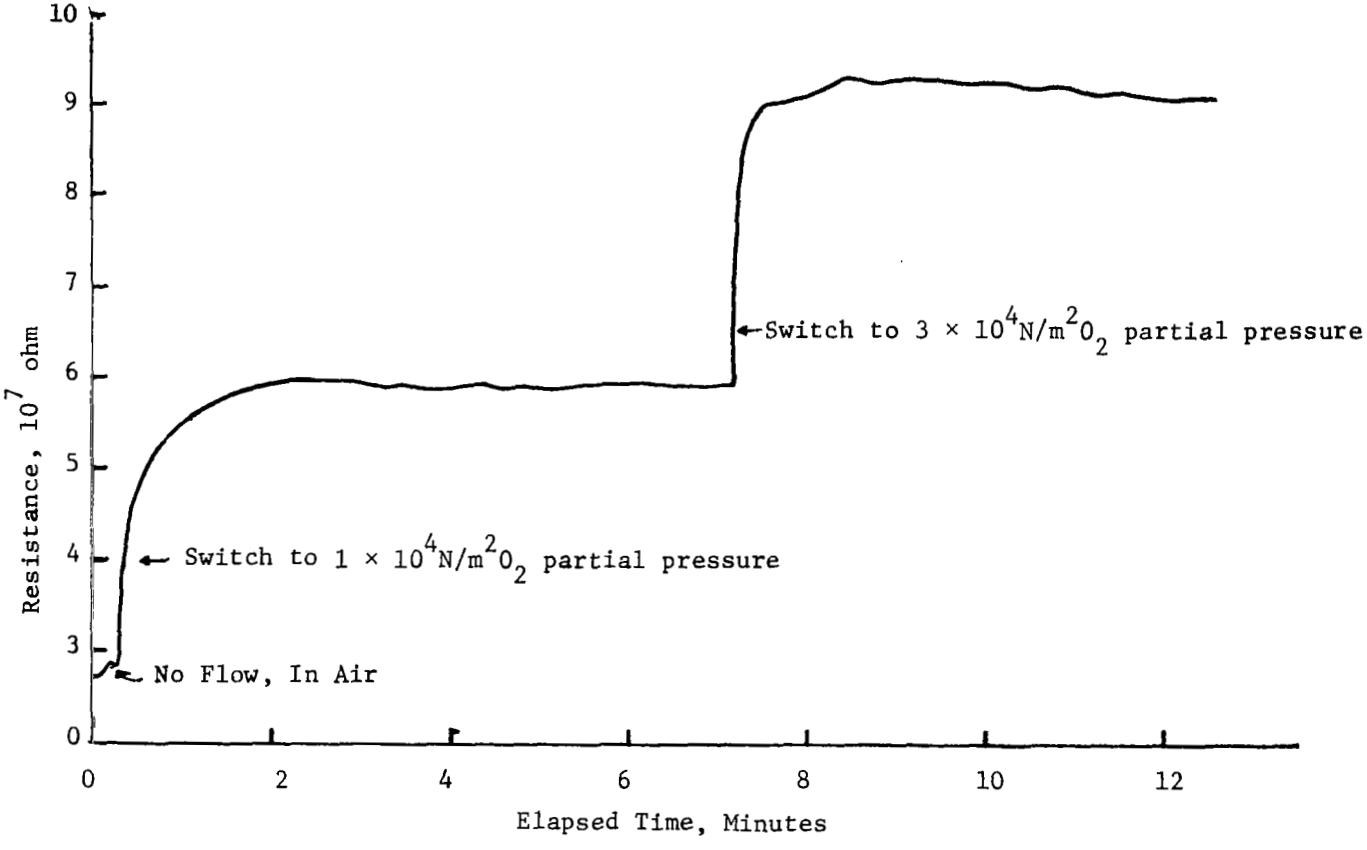

Figure 31. Resistance Versus Time Showing Response of 90 nm Sensor to Change in O_2 Content of Gas Stream.

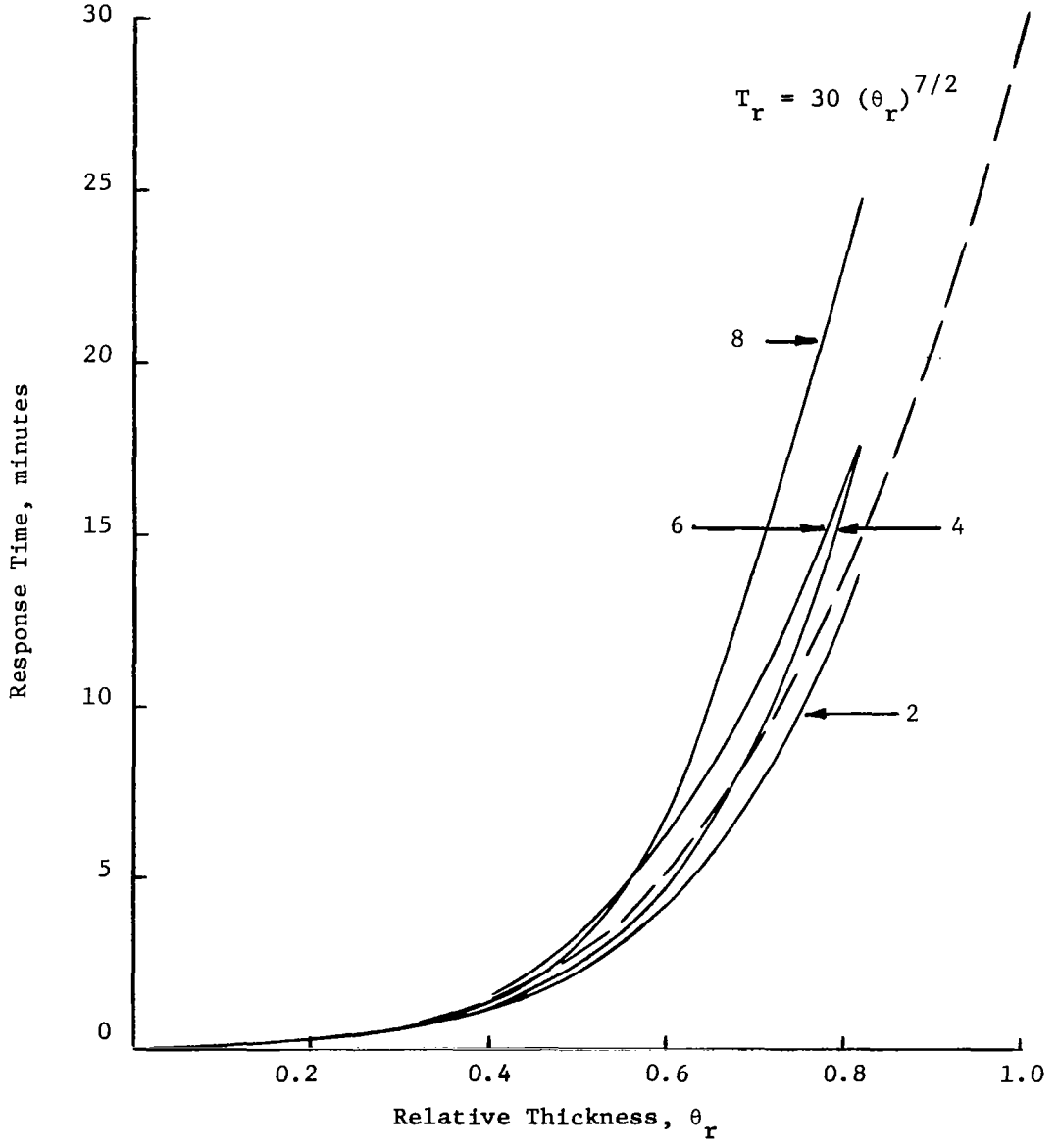

Figure 32. Response Time (10% to 90%) Versus Relative Thickness for ZnO Film Sensors. Step Size of Oxygen Partial Pressure, in $10^4 N/m^2$, is Indicated for Each Curve. Dashed Line Gives the Approximate Curve $T_r = 30\ (\theta_r)^{7/2}$.

with 360 nm taken as 1.0. The marked increase in response time may be explained by taking a porous, or permeable model, for the ZnO film, which would invoke mass transport of oxygen by diffusion to explain the long response times of the thicker films. This model is discussed in detail later in Section III.

Figure 26 shows a plot of the common logarithm of film conductance versus oxygen partial pressure for two of the sensor samples, 2B, which was 150 nm thick, and 3C, which was 210 nm thick. The shapes of the curves are typical. Both exhibit a fairly rapid decrease of conductance in the range 0 to $2 \times 10^4 N/m^2$ 0_2 partial pressure, indicating that a large fraction of the available adsorption sites are covered in this range. From 2×10^4 to $10 \times 10^4 N/m^2$ 0_2 the slope is smaller, indicating that on an incremental basis the surface is increasingly more difficult to cover. This behavior is consistent with a model in which interaction between adsorbed species is taken into account.

Response to Other Gases. - Figure 33 shows the response of one sensor 13E, 210 nm thick, to oxygen, compressed air, nitrogen, carbon dioxide and argon, all plotted together for comparison. The sputtered film appeared to be inert to N_2, Ar and CO_2.

Response to Water Vapor. - Water vapor was found to seriously affect the film response. To perform the tests the gas stream of oxygen and nitrogen was routed through a bubbler containing water at a constant temperature. An alternate route bypassed the bubbler. The input to the sensor was switched back and forth between the dry stream and wet stream, at a given bath temperature, at a given partial pressure oxygen in the gas stream. The results are shown in Figure 34. Water vapor at about 2700 N/m^2 partial pressure, inferred from the water bath temperature, in the gas stream flowing over the sensor tended to decrease the conductance of the ZnO film over the range of oxygen partial pressure from zero to $10^5 N/m^2$. This decrease is relative to the conductance exhibited by the film for a given oxygen partial pressure in a gas stream without water vapor at approximately 864 N/m^2, again inferred from water bath temperature, tended to increase ZnO film conductance at a given oxygen partial pressure. Since the water reservoir was in an ice bath to obtain the low partial pressure of water vapor, it was suspected that some thermal effects were responsible. However upon heating the vapor laden gas stream prior to the entrance, no change was noted in the behavior. Then it was suspected that the gas sources, N_2 and 0_2 contained in standard cylinder, contained water vapor. The supplier specified a water vapor content equivalent to about 206°K dew point. In order to check this N_2 was metered at 100 cc/min

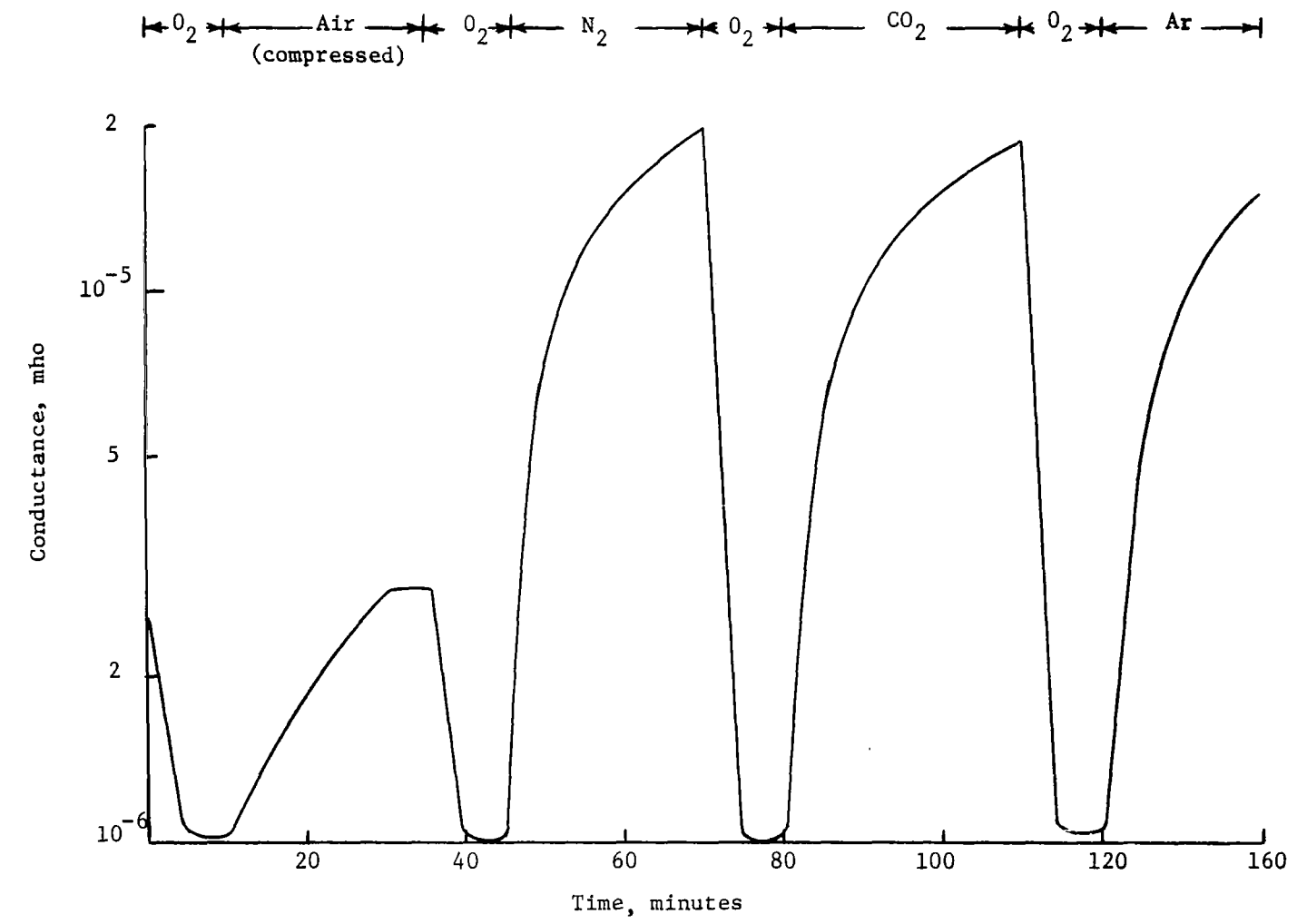

Figure 33. Response of Sensor 13E to Various Gases.

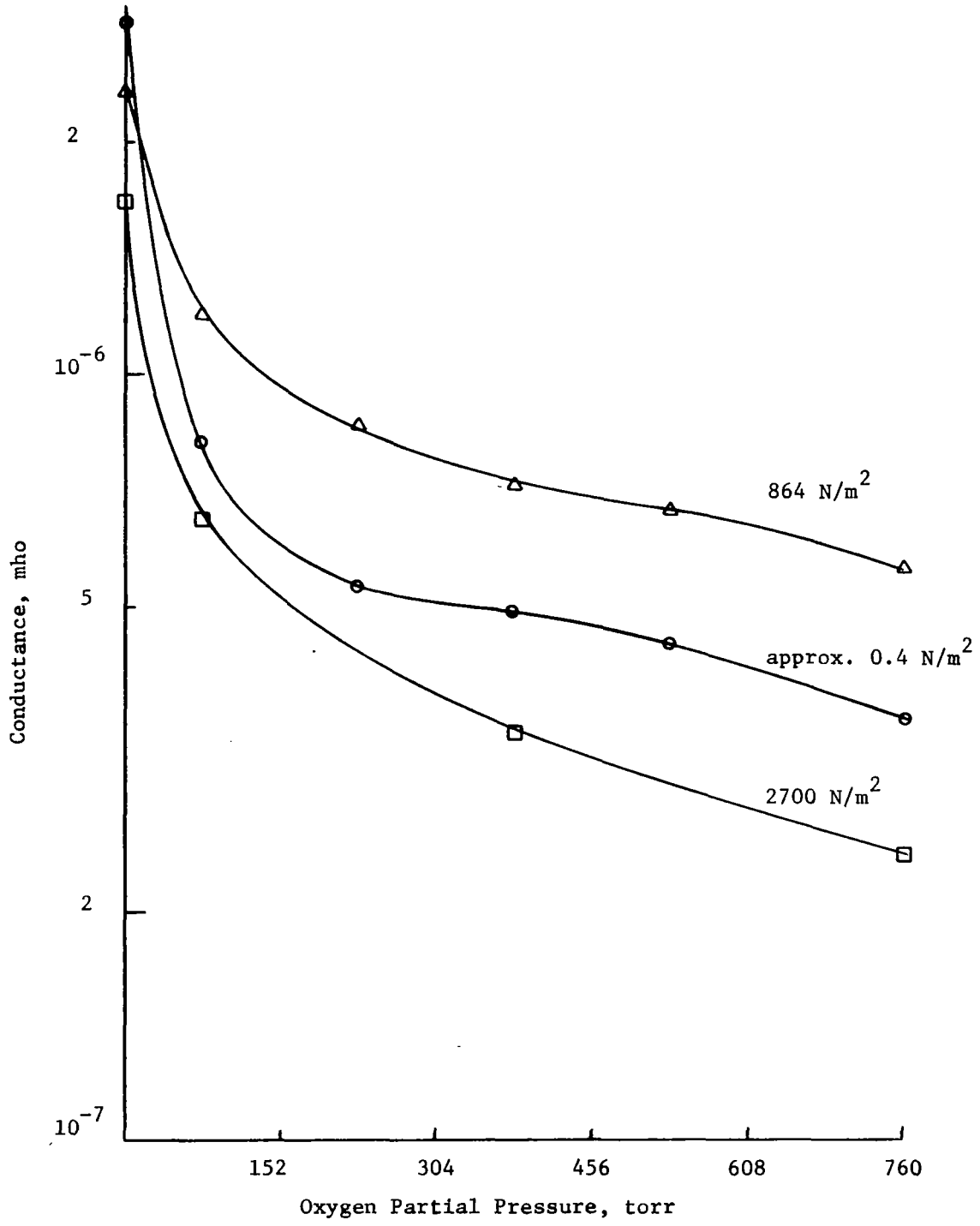

Figure 34. Effect of Water Vapor, at the Partial Pressures Shown on the Oxygen Partial Pressure Response of Sensor 2B.

through a dry ice (CO_2)-acetone cold trap for one hour. Then the side open to atmosphere was clamped shut and the "U" tube through the cold trap was withdrawn for inspection. There was some water vapor condensed on the inlet side of the cold trap, but far less than would have been transported at 864 N/m^2 partial pressure at a total flow rate of 100 cc/min for one hour. The check of the O_2 supply produced a similar result. As a consequence of these tests, the anomalous behavior with respect to low and high water vapor content could not be attributed to a residual amount in the "dry" gas supply.

In both the low and high water vapor cases, it was found that switching from "dry" gas to "wet" gas resulted in a slow drift to the steady state values. On the other hand, a change from "wet" to "dry" gas resulted in a fairly rapid change, with a response time close to that normal for the film responding to a change in oxygen content of the ambient gas. Some typical results are given in Table 5. This behavior is consistent with that noted previously for oxygen desorption. The ZnO surface, hotter than the ambient gas steam, results in a lowering of the energy barrier to desorption. In addition the characteristic vibration frequencies and amplitudes of adsorbed particles would be higher at the higher temperatures, providing an enhanced chance of escape.

Other workers have studied the effect of water vapor on various properties of zinc oxide. Nobbs [Ref. 13] found that water vapor speeded up the rate of decay of the photoconductive effect of zinc oxide. Trapnell [Ref. 7, page 211] quotes calculations by another worker on the vibrational entropy of water vapor adsorbed on zinc oxide at 630°K. This calculation is in good agreement with the entropy measured by experiment, indicating that the adsorbed water has no translational entropy. The conclusion is that the water vapor is immobile. These two observations, along with those of the present work allow a conjecture as to the mechanism of the effect of water vapor on the conductivity of zinc oxide.

The speed up of the decay rate of photoconductivity and the increase in resistance noted in the present work at a fairly high partial pressure of H_2O may be interpreted as the trapping of mobile charge carriers, probably electrons, at the surface during the chemisorption of the H_2O. The increase in resistance over the normal for a given partial pressure of oxygen is due most likely to the more or less permanent occupation of an adsorption by H_2O, due to its zero or low mobility. In contrast, for dry gas of N_2 and O_2 composition, it is probable that there is a continual interchange of site occupants due to mobility on the surface and between the gas and the surface. The resistance characteristic for a given oxygen partial pressure in a dry gas reflects a dynamic balance of these interchanges. The balance

Table 5. Response Times (10% to 90% of Total Response) for Switching Back and Forth from Wet to Dry Gas Streams.

Partial Pressure of O_2 in Stream $10^4 N/m^2$	Direction of Switching	Response Time (Minutes)
	Sample 2B 150 nm thick	
1	dry → wet	1.8
1	wet → dry	0.38
1	dry → wet	3.5
1	wet → dry	0.5
5	wet → dry	0.34
5	dry → wet	11.9
5	wet → dry	0.28
	Sample 4D 300 nm thick	
5	wet → dry	0.94
5	dry → wet	7.66
5	wet → dry	2.5
5	dry → wet	14.2

is upset, relatively slowly but inexorably by the more persistent H_2O, presumably in occupying sites previously occupied by oxygen.

Why a reduction in H_2O partial pressure to about one third of that responsible for the behavior discussed above should have an apparently opposite effect is not clear at present.

Operational Characteristics

In addition to the data presented and discussed above, engineering application requires a knowledge of the operating characteristics, primarily stability and repeatability. Accuracy is important, but depends upon the standard used for calibration. Once the sensor has been calibrated, stability and repeatability are necessary for accurate indication.

The method used for calibration in the tests for this project was to use gas sources of commercial purity and rotameter flow meters rated at $\pm$5% of full scale. When sensors were initially heated, the gas stream flowing over them was switched back and forth from nitrogen and oxygen reservoirs to check the resistance levels. The thinnest samples, which exhibited the fastest response, also exhibited a large initial drift. A 90 nm sample on initial heat-up in oxygen reached 4×10^7 ohm but in 40 minutes had drifted down to 1.6×10^7 ohm. Following a switch to N_2 and then back to oxygen, the resistance went to $5.5 \times 10^7 \Omega$ and drifted back to 1.5×10^7 in one hour. After several such cycles the overshoot in oxygen was to 1.6×10^8 ohm in two hours. The sample was left heated in O_2 overnight and the next day had about 10% drift. The same sample was removed from the test set-up until several days later, during which time it was stored in ambient air at room temperature. On the next series of tests, after about a half hour at operating temperature, drift was about 10% on low O_2 content streams and about 5% at high O_2 content.

A sample of 300 nm thickness exhibited, on initial heat-up and cycling, a change of about 30% in the resistance levels in N_2 and O_2 during the first day of operation. Subsequent drift was about 5%.

Some of the drift was attributable to changes in the gas stream composition due to regulator fluctuations in the case of mixed O_2 and N_2. This was eliminated by using a 1000 mℓ flask as a mixing chamber prior to admitting the gas stream to the sensor. However, the large scale drift observed in initial heat-up must be attributed to the sensor. It is possibly due to adsorbed material which is not easily driven off. No special chambers, such as a dessicator, were used to house the sensors prior to mounting in the housing, or in the test interims.

Theoretical Model for ZnO as an Oxygen Partial Pressure Sensor

In the following paragraphs a theoretical model is proposed to explain the major features of the behavior observed during the experiments carried out under the present project. These features are:

1. The increase of resistance and the change in the nature of the source of mobile charge carriers when a sputtered zinc oxide film is annealed at a high temperature in an atmosphere with an appreciable oxygen content.

2. The change in resistance of a heated zinc oxide film, which has been annealed at higher temperature than the operating temperatures, when the oxygen content of the ambient gas is increased or decreased.

3. The shape of the resistance versus oxygen partial pressure curve at a constant temperature.

4. The transient response characteristics of the sputtered zinc oxide film.

The annealing process is carried out in an atmosphere with appreciable oxygen content. The gas is in thermal equilibrium with the zinc oxide. If sufficient time is allowed for the process the electrical resistance of the film is increased and the slope of the log R versus reciprocal temperature is increased. The model assumed for this behavior is a zinc rich material prior to annealing with the zinc located interstitially in the lattice.

At the elevated annealing temperature interstitial zinc, Zn_i, near the oxygen rich surface in contact with the gas phase is combined with adsorbed oxygen. This creates a concentration gradient which promotes the flow of Zn_i, by diffusion, to the surface. Since it is highly probable that adsorbed oxygen traps an electron, it seem likely that the electric field created by adsorbed oxygen would tend to enhance diffusion of ionized zinc interstitials, Zn_i^+, toward the surface. Norman [Ref. 14] has reported work in which zinc oxide powder was heated in air for 2 1/2 hours at temperatures ranging from 273°K to 1073°K. The powder which contained a large amount of excess zinc was found to undergo a large decrease in excess zinc content starting at about 523°K. At 773°K of the excess zinc originally present. Similar results were found by Allsopp and Roberts [Ref. 15] who heated zinc powder in pure oxygen for 1/2 hour.

The reaction taking place at the surface is assumed to be

$$Zn_i^+ + e + 1/2\ O_2 \rightleftarrows ZnO \ . \tag{18}$$

The equilibrium constant for this reaction is

$$K_1 = \frac{[ZnO]}{[Zn_i^+][e][O_2]^{1/2}} \tag{19}$$

where the square brackets indicate the concentrations of the reactant species. These concentrations are the surface concentrations since it is at the surface where the reaction occurs. The surface concentration of oxygen is determined by the partial pressure of oxygen in the ambient gas, p_{O2}, the gas temperature, T_G, and the surface temperature, T_s. It is also influenced by the presence of other gases and their adsorption characteristics, since molecules of other gases are in competition for surface sites.

From equation (19), the amount of ZnO at the surface is given by

$$[ZnO] = K_1[Zn_i^+][e][O_2]^{1/2} \ . \tag{20}$$

In this form it is apparent that if there is a high concentration of electrons, due perhaps to other donor species than zinc interstitials, the tendency is to increase the surface concentration of ZnO and deplete the interstitial zinc concentration until the balance implied by the equilibrium equation (20) is reached. Of course, this assumes an unlimited supply of oxygen relative to the interstitial zinc. However, if interstitial zinc is the only donor source the equilibrium equation

$$\frac{1}{K_2}\ [Zn_i] = [Zn_i^+]\ [e] \tag{21}$$

must hold and equation (20) may be re-written as

$$\frac{[ZnO]}{[Zn_i]} = \frac{K_1}{K_2}\ [O_2]^{1/2} \ . \tag{22}$$

Since the equilibrium constants K_1 and K_2 depend upon the change in free energy of the respective reactions and upon the temperature in the form

$$K = \exp\ (\Delta\mu/kT) \tag{23}$$

where $\Delta\mu$ is the change in free energy and T is the temperature, equation (22) can be put into the form

$$\frac{[ZnO]}{[Zn_i]} = [O_2]^{1/2}\exp(\Delta\mu/kT)\ . \tag{24}$$

This states that at equilibrium there is a fixed ratio of the concentration of ZnO to interstitial zinc. This ratio depends upon the surface concentration of oxygen, hence upon the ambient partial pressure of oxygen, and upon the temperature.

Consider a slab of ZnO of unit surface area and thickness d. The number of sites at the surface is N_s and the volume concentration of Zn_i prior to annealing is n_o per cc. The number of Zn_i in the slab is $n_o d$. The ratio of surface sites to the number interstitials in the bulk is

$$r_{SB} = N_s/n_o d \tag{25}$$

the order of magnitude of N_s is 10^{15} for 1 cm^2 area. For an interstitial density of 10^{17} per cc and a thickness of 90 nm, $n_o d = 9 \times 10^{11}$ and, therefore, $r_{sB} \approx 275$. The depletion of Zn_i by diffusion to the surface changes, the surface concentration of ZnO to only a very slight degree and from (24) one would, therefore, expect the remaining concentration of Zn_i to be the same for films of the same order of magnitude of thickness, such as those used the present work.

If the annealing temperature and oxygen partial pressure are sufficiently large, the number of Zn_i remaining should be small. Then the bulk donor concentration no longer dominates the electrical behavior. This leads to the introduction of the next assumption. This is: the donor species is located at the surface of the zinc oxide, and is most likely due to the disruption of a Zn-O bond. This reaction is the inverse of the one leading to a ZnO formation at the surface. It would permit oxygen to leave the surface and enter the gas phase, leaving behind free zinc to

ionize and free an electron into the conduction band. The ionization energy of the zinc would be small compared to the bond disruption energy which dominates the process. The ionized zinc would tend to diffuse away from the surface, but if the temperature is not too high the diffusion constant would not be large enough to cause a rapid migration. Thus, if the oxygen partial pressure in the ambient gas is increased, the electrons can be retrapped at the surface and the zinc and oxygen recombined, so that the behavior is reversible. It must be emphasized that the Zn-O bond postulated at the surface is characterized by a lower energy, on the order of 0.3 eV, than that of Zn-O bonds in the bulk. This is attributable to the fact that a zinc atom at the surface is already bonded to oxygen atoms in the next layer down, whereas an oxygen atom attached to the surface zinc atom will not be likely to be surrounded by zinc atoms. Thus it will not make multiple bonds.

The next assumption of the model is that the surface of the zinc oxide film is extended by micropores. This assumption is invoked to explain the rapid increase in response time with thickness. Bickerman [Ref. 16, Chapter 7] has pointed out that sorption on zeolites, which exhibit an extensive microporosity, is probably indicative of what happens in the case of other apparently solid surfaces. It should be pointed out here that photographs made with an electron microscope did not show any structure which could be constued as micropores on unannealed ZnO films. However, on films annealed oxygen at a very high temperature, 1173°K, the surface appeared mottled indicating non-uniform structure. As shown in Appendix A, a model which assumes a permeable medium characterized by a diffusion constant D can lead to a quadratic dependence of response time on thickness.

The shape of the conductance versus oxygen partial pressure curve, with typical examples shown in Figure 26, can be explained as follows. First, a re-plot of the data on log-log coordinates, as shown in Figure 35, reveals an approximate square root dependence of the conductance decrease is assumed to be the depletion of conduction band electronics due to trapping at the surface by adsorbed oxygen, the change in the conduction band electron population must be proportional to the square root of the oxygen partial pressure. From equation (24) the ratio of $[ZnO]/[Zn_i]$ is dependent upon the square root of the surface concentration of O_2. Thus the number of disrupted Zn-O bonds at the surface, and, by assumption, the number of free electrons should decrease as the square root of the O_2 surface concentration. It follows that the surface concentration of O_2 is directly proportional to the O_2 partial pressure in the gas in contact with the surface. Therefore,

$$[O_2]_{surface} = A\, p_{O2} \tag{26}$$

where $[O_2]_{surface}$ is the surface O_2 concentration, A is a proportionality

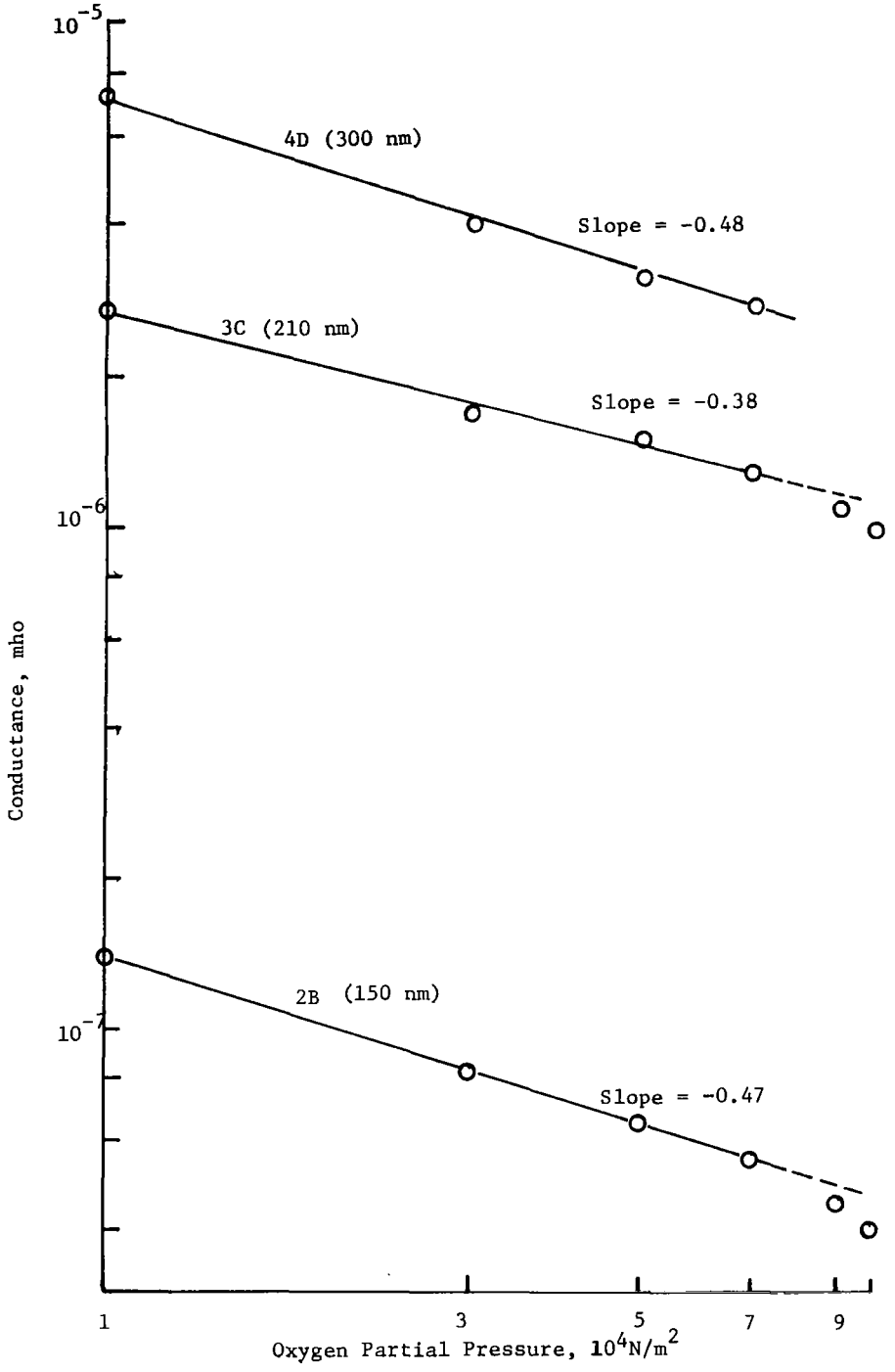

Figure 35. Conductance Versus Oxygen Partial Pressure for Three Samples Showing Approximate Square Root Dependence of Conductance Upon Pressure.

constant and p_{02} is the partial pressure of O_2 in the gas in contact with the surface.

As shown in Appendix B a model with two gases competing for adsorption sites on the surface can lead to such a linear relation between the fraction of sites covered by one of the gases and the partial pressure of the gas when the two gases have similar adsorption characteristics. Since

$$[O_2]_{surface} = \theta_{02} n_s \tag{27}$$

where n_s is the number of sites per unit area, and

$$\theta_{02} \simeq \frac{p_{02}}{p_T} \tag{28}$$

where p_T is the total pressure, then

$$[O_2]^{1/2}_{surface} = \left(\frac{n_s}{p_T}\right)^{1/2} p_{02}^{1/2} \tag{29}$$

Thus, the number of carriers should decrease as the square root of the O_2 partial pressure.

SECTION IV

CONCLUSIONS

The work reported above has demonstrated the feasibility of fabricating a miniature oxygen partial pressure sensor using sputtered zinc oxide films. These were tested over the range from zero to about $10^5 N/m^2$ (760 torr) partial pressure of oxygen. They were found to be relatively inert to nitrogen, carbon dioxide and argon gases, but water vapor was found to change the characteristics to an important degree, indicating that a dessicant should be used to remove water vapor from the input gas stream in order to assure reliable operation.

The power consumption required to maintain the sensor at the operating temperature of about 670°K required for optimum response was about 2.5 watts. By using 4 ohm-cm p-type silicon, reliable high temperature contacts could be made to the heater bar and the ZnO film and the current required could be kept at levels on the order of 100 ma. A reliable insulation for high temperature operation was found and used.

Film thickness was found to be an important factor in the response time. Sensors with film thicknesses of about 90 nm exhibited 10% to 90% response times of 20 to 30 seconds to step changes in oxygen partial pressure. Response time increased markedly with increase in film thickness but the sensitivity, in terms of the change in conductance divided by the base conductance (no oxygen) was found to be about the same for the range of film thicknesses tested.

When first put into operation the sensors exhibit a drift in characteristics. After an induction period of several hours at the operating temperature the performance stabilizes to give a reproducible response to oxygen partial pressure. The cause of the drift is not known, but it may be due to strongly adsorbed impurities.

Control circuitry for maintaining a stable heater temperature and circuits to condition the signal to provide an approximately linear output were developed and packaged to provide a laboratory model of an oxygen partial pressure sensor when used with the thin film zinc oxide sensing elements developed in this project.

Appendix A

PERMEABLE SLAB MODEL FOR ZnO FILM RESPONSE TO OXYGEN

In order to explain the increase in response time with thickness of sputtered ZnO films, a permeable model is used. The geometry is sketched below

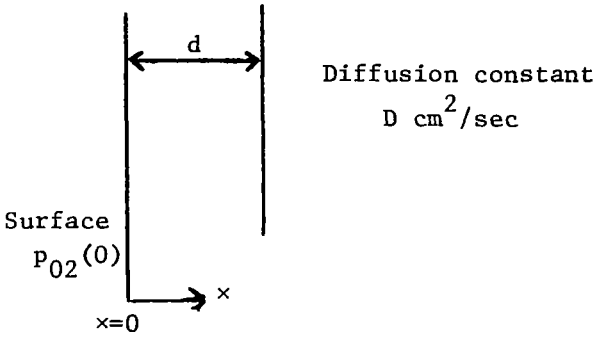

The permeable material is characterized by a diffusion constant D which enters the Fick's law equation for diffusion as

$$\frac{\partial c}{\partial t} = D \frac{\partial^2 c}{\partial x^2} \qquad \text{(A-1)}$$

where $c = c(x,t)$ is the concentration of the diffusing component at distance x into the material at time t. This equation can be solved using the boundary condition that the concentration remains constant at the surface, $x = 0$, for all time greater than $t = 0$. For convenience the initial concentration is taken as $c(x,0) = 0$ throughout the slab, although a constant can be added to the solution and the surface concentration, c_0, expressed as the difference, Δc, between the impressed surface concentration and the existing background concentration. The solution of (A-1) subject to the boundary conditions

$$c(0,t) = c_0 \qquad t>0$$

$$c(x,0) = 0$$

is

$$c(x,t) = c_0[1-\text{erf}(x/2\sqrt{Dt})] \tag{A-3}$$

where

$$\text{erf } \xi = \frac{2}{\sqrt{\pi}} \int_0^x \exp(-\xi^2) d\xi \tag{A-4}$$

is the Gauss error function. This function has the limiting values

$$\begin{aligned} \text{erf}(0) &= 0 \\ \text{erf}(\infty) &= 1 \end{aligned} \tag{A-5}$$

The solution (A-3) and the properties of the error function are described in many texts. See for example, W. Jost [Ref. 17].

Assuming that O_2 behaves as a perfect gas, the partial pressure is directly proportional to the concentration of O_2. Therefore, the solution (A-3) can be re-written in terms of the partial pressure, $p_{02}(x,t)$ of O_2 at depth x, in the material and at time t, given a surface (x = 0) pressure of $p_{02}(0)$

$$p_{02}(x,t) = p_{02}(0)[1 - \text{erf}(x/2\sqrt{Dt})] \quad . \tag{A-6}$$

As shown in Appendix B, for a gas mixture of O_2 and N_2, assuming similar adsorption and desorption activation energies, the fractional coverage of O_2 on the surface is given approximately by

$$\theta(x,t) \simeq \frac{1}{p_T} p_{02}(x,t) \tag{A-7}$$

where p_T is the total pressure.

In this relation, the concept of a surface is extended to the region throughout the slab where the O_2 gas is in contact with solid ZnO.

The average coverage throughout the slab at time t is given by

$$\theta(t) = \frac{1}{d} \int_0^d \theta(x,t) dx \tag{A-8}$$

or

$$\bar{\theta}(t) = \frac{p_{02}(0)}{d\ p_T} \int_o^d [1 - \text{erf}\ \frac{x}{2\sqrt{Dt}}]dx \qquad \text{(A-9)}$$

The integral of the error function cannot be given in closed form, but an approximation can be obtained by using series expansions. Since

$$\exp(-\xi^2) = 1 - \xi^2 + \frac{\xi^4}{2} - \cdots , \qquad \text{(A-10)}$$

and

$$\text{erf}\ y = \frac{2}{\sqrt{\pi}} \int_o^y (1 - \xi^2 + \frac{\xi^4}{2} - \ldots)d\xi , \qquad \text{(A-11)}$$

then

$$\text{erf}\ y = \frac{2}{\sqrt{\pi}}(y - \frac{y}{3} + \frac{y^5}{10} - \ldots) . \qquad \text{(A-12)}$$

Now

$$\int_o^g \text{erf}\ y\ dy = \frac{2}{\sqrt{\pi}}(\frac{g^2}{2} - \frac{g^4}{12} + \frac{g^6}{60} - \cdots). \qquad \text{(A-13)}$$

With the substitution

$$\int_o^d \text{erf}\ \frac{x}{2\sqrt{Dt}}\ dx = 2\sqrt{Dt} \int_o^{d/2\sqrt{Dt}} \text{erf}\ \frac{x}{2\sqrt{Dt}}\ d\ \frac{x}{2\sqrt{Dt}}$$

equation (A-9) can be integrated to obtain

$$\bar{\theta}(t) = \frac{p_{02}(0)}{dp_T} \left[d - \frac{4\sqrt{Dt}}{\sqrt{\pi}} \left(\frac{d^2}{8Dt} - \frac{d^4}{192D^2t^2} + \ldots\right)\right]$$

or

$$\bar{\theta}(t) = \frac{p_{02}(0)}{p_T} \left[1 - \frac{1}{\sqrt{\pi}} \left(\frac{d}{2\sqrt{Dt}} - \frac{d^3}{48(Dt)^{3/2}} + \ldots\right)\right] \qquad \text{(A-14)}$$

The higher order terms in $d/2\sqrt{Dt}$ have rapidly decreasing coefficients. To a good approximation

$$\theta(t) \simeq \frac{p_{02}(0)}{p_T} \left(1 - \frac{d}{\sqrt{4\pi Dt}}\right) \qquad \text{(A-15)}$$

From this equation it can be seen that doubling the slab thickness d requires four time as much time to reach the same degree of coverage.

APPENDIX B

RELATION OF SURFACE COVERAGE TO PARTIAL PRESSURE FOR A TWO GAS MIXTURE

In the theory of adsorption it is customary to use the symbol Θ to denote the fractional coverage of gas on a surface. If there are n_s surface sites for adsorption per cm^2 and n_c per cm^2 are covered by the adsorbed gas at a given time

$$\Theta = n_c/n_s \tag{B-1}$$

The relation between Θ and the pressure of a gas in contact with an adsorbing surface has been considered by many authors. Trapnell [Ref. 8, Chapter V] considers in detail the models used to derive some of the various expressions for Θ as a function of gas pressure at a constant temperature. These are termed "isotherms". They are derived assuming thermal equilibrium between the gas and the adsorbent surface. The kinetic method of derivation sets up an expression for the rate at which gas particles are incident on the surface, u (particles/sec), and an expression for the rate at which they leave the surface, u' (particles/sec). At equilibrium the two rates are equal. From this equality and by assuming a reasonable relation between u and Θ, and between u' and Θ, the dependence of Θ upon the gas pressure can be derived.

In the work reported here the ZnO surface was not in thermal equilibrium with the surrounding gas, since heat was dissipated by the surface to the gas. However, a dynamic equilibrium is reached when the oxygen content of the gas is constant in time and the dissipation rate of heat from the sensor is constant. The kinetic approach can be used to derive an expression relating Θ, the fractional surface coverage, to p, the partial pressure of the gas being adsorbed. Following Trapnell [Ref. 8, page 110 *et seq.*], the adsortpion rate can be written as

$$u = \frac{p}{\sqrt{2\pi m k T_G}} \cdot \sigma \cdot f(\Theta) \cdot \exp\left(\frac{-E_A}{kT_G}\right) \tag{B-2}$$

where p is the gas pressure, m the gas molecule mass, k is Boltzmann's constant, T_G the gas temperature, σ the condensation coefficient, $f(\Theta)$ a function dependent upon the degree of coverage of the surface, and E_A is an activation energy for adsorption. The first factor in parentheses in equation (B-2) gives the rate at which gas molecules are incident upon the surface at a given gas temperature, T_G, and pressure p. A typical

order of magnitude for this rate for O_2 molecules at $10^5 N/m^2$ and 300°K is 3×10^{23} per cm^2 per second incident upon the surface. The value of σ is typically near 1.0.

The rate of desorption from the surface is given by

$$u' = B \cdot f'(\Theta) \cdot \exp\ (-E_D/kT_s) \qquad \text{(B-3)}$$

where B is the desorption velocity constant, $f'(\Theta)$ a function of the degree of surface coverage, T_s is the surface temperature and E_D the activation energy for desorption of a gas molecule from the surface. The value of B is dependent upon the type of gas, the type of surface; and, often, the degree of coverage. A theoretical estimate ignoring these complications as given by Trapnell [Ref. 8, page 94] is about 10^{28} per cm^2 per second.

Another complication, which is not covered in the text cited, is the presence of two types of gas molecules, N_2 and O_2, in the gas used in the tests reported here. These compete for adsorption sites on the ZnO surface. If an N_2 molecule occupies an adsorption site, an oxygen molecule presumably cannot get close enough on this site to tie up an electron and initiate a bonding mechanism. The effect of the presence of a second gas species can be analyzed by introducing subscripts 1 and 2 in equations (B-2) and (B-3) to obtain

$$u_1 = \frac{p_1}{\sqrt{2\pi m_1 kT}}\, \sigma_1 f(\Theta_1,\Theta_2)\, \exp\ \frac{-E_{A1}}{kT_G} \qquad \text{(B-4)}$$

$$u_2 = \frac{p_2}{\sqrt{2\pi m_1 kT_G}}\, \sigma_2 f(\Theta_1,\Theta_2)\, \exp\ \frac{-E_{A2}}{kT_G} \qquad \text{(B-5)}$$

$$u_1' = B_1 f'(\Theta_1)\, \exp\ (-E_{D1}/kT_s) \qquad \text{(B-6)}$$

$$u_2' = B_2 f'(\Theta_2)\, \exp\ (-E_{D2}/kT_s). \qquad \text{(B-7)}$$

The symbols have the same meaning as before with the subscripts denoting the quantities applicable to species 1 or 2. For example p_1 is the partial pressure of species 1, and Θ_1 is the fraction of adsorption sites covered by species 1, and so forth.

If it is assumed that the rate of adsorption of species 1 and 2 is proportional to the fraction of surface sites not covered, or

$$f(\Theta_1,\Theta_2) = 1 - \Theta_1 - \Theta_2 \tag{B-8}$$

and the rate of desorption of molecule types 1 and 2 is proportional to the fraction of sites covered by the respective species, or

$$f'(\Theta_1) = \Theta_1 \tag{B-9}$$

$$f'(\Theta_2) = \Theta_2 \tag{B-10}$$

then at equilibrium balancing of the adsorption and desorption rates of the separate species, using equations (B-4) through (B-10) yields

$$\frac{(1 - \Theta_1 - \Theta_2)}{\sqrt{2\pi kT_G}} = \frac{B_1\Theta_1\sqrt{m_1}}{p_1\sigma_1} \exp\,(E_{A1}/kT_G - E_{D1}/kT_s) \tag{B-11}$$

and

$$\frac{(1 - \Theta_1 - \Theta_2)}{\sqrt{2\pi kT_G}} = \frac{B_2\Theta_2\sqrt{m_2}}{p_2\sigma_2} \exp\,(E_{A2}/kT_G - E_{D2}/kT_s). \tag{B-12}$$

A simplifying assumption is introduced at this point, namely, that the condensation coefficients and the desorption velocity constants are the same for both species. If this is true, equating (B-11) and (B-12) gives

$$\frac{\Theta_2}{\Theta_1} = \frac{p_2}{p_1} \quad \frac{m_1}{m_2} \exp \frac{E_{A2} - E_{A1}}{kT_G} \quad \exp \quad \frac{E_{D1} - E_{D2}}{kT_s} \tag{B-13}$$

Define

$$\Delta E_A = (E_{A2} - E_{A1}), \tag{B-14}$$

$$\Delta E_D = (E_{D2} - E_{D1}), \tag{B-15}$$

and

$$M = \frac{m_1}{m_2} \exp \frac{\Delta E_A}{kT_G} \exp \frac{-\Delta E_D}{kT_s} \quad . \tag{B-16}$$

Then

$$\Theta_2 = M \frac{p_2}{p_1} \Theta_1 \tag{B-17}$$

Substituting this unto equation (B-11) gives

$$\frac{\Theta_1}{1 - (1 + Mp_2/p_1)\Theta_1} = c_1 p_1 \tag{B-18}$$

where c_1 is defined by

$$c_1 = \frac{\sigma_1}{B_1\sqrt{2\pi m_1 kT_G}} \exp \frac{E_{D1}}{kT_s} - \frac{E_{A1}}{kT_G} \quad . \tag{B-19}$$

Now equation (B-18) can be solved for Θ_1 in terms of the pressures p_1 p_2. This gives

$$\Theta_1 = \frac{c_1 p_1}{1 + c_1 p_1 + Mc_1 p_2} \tag{B-20}$$

If M is on the order of unity, implying that the differences in adsorption and desorption activation energy are very small for the two species, and the quantities $c_1 p_1$ and $Mc_1 p_2$ are both much larger than unity

$$\Theta_1 \simeq \frac{p_1}{p_1 + p_2} \tag{B-21}$$

The coverage is directly proportional to the partial pressure.

Another possibility is that, although the adsorption energies are about equal, the desorption activation energy of component 1 is much larger than that of component 2. This might be expected if component 1 is chemisorbed and component 2 is physically adsorbed. In this case

$$\Theta_1 \simeq \frac{1}{M} \; p_1/p_2 \tag{B-22}$$

Since the sum of the partial pressures gives the total pressure, or

$$p_T = p_1 + p_2 \tag{B-23}$$

Then

$$\theta_1 \simeq \frac{1}{M} \frac{p_1}{p_T - p_1} \tag{B-24}$$

Again, for p_1 small this gives an approximately linear relation between the coverage θ_1 and the gas partial pressure p_1.

REFERENCES

1. Burger, R. M.; Canady, K. S.; and Wortman, J. J.: "A Study of Thin Film Partial Pressure Gas Sensors", NASA CR-66306, Prepared under Contract No. NAS1-5891, Research Triangle Institute, 1967.

2. Royal, T. M.; Wortman, J. J.; and Monteith, L. K.: "An Investigation to Thin Film Oxygen Partial Pressure Sensors", NASA CR-1182, Research Triangle Institute, 1968.

3. Pearson, C. R.: "Feasibility of Miniaturizing a Heater for a Thin-Film Oxygen Partial Pressure Sensor", NASA TN-D6134, 1971.

4. Pearson, C. R.: "The Development of a Miniaturized Heater for Thin Film Oxygen Partial Pressure Sensors", Master's Thesis, University of Virginia, 1969.

5. Kroger, F. A.: "The Chemistry of Imperfect Crystals", North Holland Publishing Company, Amsterdam, 1964.

6. Tischer, G.: Data given in Figure 36, Page 248 of the article cited below as Reference 10.

7. Trapnell, B. M. W.: "Chemisorption", Butterworths Scientific Publications, London, 1955.

8. Peierls, R: "Statistical Theory of Adsorption with Interaction Between the Adsorbed Atoms", Proc. Camb. Phil. Soc., Vol. 32, 471-476, 1936.

9. Bevan, D. J. M.; and Anderson, J. S.: "Electronic Conductivity and Surface Equilibria of Zinc Oxide", Disc. Faraday Soc., Vol. 8, 238, 1950.

10. Heiland, G.; Mollwo, E.; and Stockmann, F.: "Electronic Processes in Zinc Oxide", p. 191-323, in "Solid State Physics, Vol. 8", edited by F. Seitz and D. Turnbull, Academic Press, New York, 1959.

11. Volkenshtein, F. F.: "The Electronic Theory of Catalysis on Semiconductors", translated by N. G. Anderson, edited by E. J. H. Birch, The MacMillan Company, New York, 1963.

12. Burger, R. M.; and Donovan, R. P.: "Fundamentals of Silicon Integrated Device Technology, Vol. I, Oxidation, Diffusion and Epitaxy", Prentice-Hall, Inc., Englewood Cliffs, N. J., 1967.

13. Nobbs, J. McK.: "The Effect of Water Vapor on the Photoconductivity of Zinc Oxide", J. Phys. Chem. Solids, Vol. 29, 439-450, 1968.

14. Norman, V. J.: "The Distribution of Interstitial Zinc in Zinc Oxide", Austr. J. Chem., Vol. 20, 85-91, 1967.

15. Allsopp, H. J.; and Roberts, J. P.: "Trans. Faraday Soc., Vol. 55, 1386, 1959. Cited in Ref. 14 above.

16. Bickerman, J. J.: "Physical Surfaces", Academic Press, New York, 1970.

17. Jost, W.: "Diffusion in Solids, Liquids and Gases", Third Printing with Addendum, Academic Press, New York, 1960.

NASA-Langley, 1972 —— 14 CR-1941